Constitutive androstane receptor directs T cell adaptation to bile acids in the small intestine

Mei Lan Chen[1,2#], Xiangsheng Huang[3#], Hongtao Wang[3], Courtney Hegner[1,2], Yujin Liu[1], Jinsai Shang[4], Amber Eliason[1], HaJeung Park[5], Blake Frey[6], Guohui Wang[3], Sarah A. Mosure[1,2,4], Laura A. Solt[1,4], Douglas J. Kojetin[4,7], Alex Rodriguez-Palacios[8,9], Deborah A. Schady[10], Casey T. Weaver[6], Matthew E. Pipkin[1], David D. Moore[11]*, and Mark S. Sundrud[1]*

[1]Department of Immunology and Microbiology, The Scripps Research Institute, Jupiter, FL 33458, USA

[2]Skaggs Graduate School of Chemical and Biological Sciences, The Scripps Research Institute, Jupiter, FL, 33458, USA.

[3]Department of Pediatrics, Section of Gastroenterology, Baylor College of Medicine and Texas Children's Hospital, Houston, TX, 77030, USA

[4]Department of Integrative Structural and Computational Biology, The Scripps Research Institute, Jupiter, FL 33458, USA

[5]X-ray Crystallography Core Facility, The Scripps Research Institute, Jupiter, FL 33458, USA

[6]Department of Pathology, University of Alabama at Birmingham, Birmingham, AL 35203, USA

[7]Department of Molecular Medicine, The Scripps Research Institute, Jupiter, FL 33458, USA

[8]Division of Gastroenterology and Liver Disease, School of Medicine, Case Western Reserve University, Cleveland, Ohio 44106, USA

[9]University Hospitals Research and Education Institute, University Hospitals Cleveland Medical Center, Cleveland, Ohio 44106, USA

[10]Department of Pathology and Immunology, Texas Children's Hospital, Baylor College of Medicine, Houston, TX, 77030, USA.

[11]Department of Molecular and Cellular Biology, Baylor College of Medicine, 1 Baylor Plaza, Houston, Texas 77030, USA

[#]Equal contribution

*Correspondence: David D. Moore (moore@bcm.edu), Mark S. Sundrud (msundrud@scripps.edu)

Key words: IBD, T cells, Th1, Th17, bile acids, MDR1, CAR, NR1I3, xenobiotics

Abbreviations: MDR1, multidrug resistance 1; TNFα, tumor necrosis factor alpha; IFNγ, interferon gamma; IL-10, interleukin-10; IL-17, interleukin-17; TCR, T cell receptor; *Abcb1a*, ATP-binding cassette subfamily B, member 1a; *Abcb1b*, ATP-binding cassette subfamily B, member 1b; *Rag1*, recombination-activating gene 1; *Rag2*, recombination-activating gene 2.

Bile acids (BAs) are fundamental lipid emulsifying metabolites synthesized in hepatocytes and maintained *in vivo* through enterohepatic circulation between the liver and small intestine[1]. As detergents, BAs can cause toxicity and inflammation in enterohepatic tissues[2], and several nuclear receptors have evolved to detoxify BAs in hepatocytes and enterocytes[3]. By contrast, it is unclear how mucosal immune cells protect themselves from high BA concentrations in the small intestine. We previously reported that CD4$^+$ T effector (Teff) cells upregulate expression of the xenobiotic transporter MDR1 in the ileum to prevent BA toxicity and suppress Crohn's disease-like small bowel inflammation[4]. Here, we identify the nuclear xenobiotic receptor, constitutive androstane receptor (CAR/*NR1I3*), as a transcriptional regulator of MDR1 expression in mucosal T cells. CAR promoted large-scale transcriptional reprogramming in Teff cells infiltrating the small intestine lamina propria (siLP), but not the colon. CAR activation by non-BA components in bile not only induced expression of detoxifying enzymes and transporters in siLP T cells, as in hepatocytes, but also the key anti-inflammatory cytokine, *Il10*. Accordingly, CAR-deficiency in T cells exacerbated, whereas pharmacologic CAR activation suppressed, BA-driven ileitis in T cell-reconstituted *Rag*$^{-/-}$ mice. These data suggest that CAR acts locally in small intestinal T cells to direct a unique transcriptional response that detoxifies BAs and fosters inflammation-resolution. Pharmacologic activation of this program offers an unexpected strategy to treat small bowel Crohn's disease.

In seeking to define transcriptional mechanisms that promote MDR1 upregulation in siLP Teff cells to safeguard small bowel immune homeostasis in the presence of BAs[4], we considered the ligand-regulated nuclear receptors (NRs), which act as environmental sensors to regulate diverse gene expression programs important for immunity, inflammation, metabolism and gastrointestinal physiology[5]. To test the contribution of each of the 49 mouse NRs to MDR1 regulation in siLP Teff cells, we performed a pooled *in vivo* RNAi screen using MDR1-dependent rhodamine 123 (Rh123) efflux[6] as a readout. Naïve CD4$^+$ T cells on the FVB/N (FVB) background were activated and transduced *in vitro* with a library of 258 mouse retroviruses carrying shRNAmirs against 70 genes together with the fluorescent reporter, ametrine (**Fig. 1a**). In addition to NRs, this library included shRNAmirs against 10 major NR co-activators and co-repressors, the aryl hydrocarbon receptor (AhR), the cell-surface BA receptor Takeda G-coupled protein receptor 5 (Tgr5; encoded by *Gpbar1*)[7] and its downstream transcription factor (*Creb1*), as well as a number of positive (*Abcb1a*, *Abcb1b*) and negative (*Cd8a*, *Cd19*, *EGFP*, *RFP*) control genes (Supplemental Table 1). Separately-transduced T cells were pooled, FACS-sorted for ametrine expression and transplanted into syngeneic *Rag1*$^{-/-}$ mice. Six-weeks later, transduced Teff cells were recovered by FACS-sorting from spleen or siLP, and portions of these cells

65 were sub-divided into MDR1^{hi} or MDR1^{lo} subsets based on *ex vivo* Rh123 efflux; relative shRNAmir
66 abundances within each cell pool were quantified by DNA-seq (**Fig. 1a**).
67 Three sets of shRNAmirs—against thyroid hormone receptor alpha (*Thra*), estrogen related
68 receptor alpha (*Esrra*), and constitutive androstane receptor (CAR/*Nr1i3*)—were most strongly and
69 consistently enriched in MDR1^{lo} *vs*. MDR1^{hi} Teff cells from both spleen and siLP, similar to shRNAmirs
70 against MDR1 (*Abcb1a*) itself, and after excluding 36 shRNAmirs that either markedly reduced Teff cell
71 persistence *in vivo* or that were poorly represented (before and after *in vivo* transfer) (**Fig. 1b**; Extended
72 Data Fig. 1a-b). This suggested that *Thra, Esrra* and CAR/*Nrli3* might each be positive regulators of
73 MDR1 expression, although none have known functions in T cells. We prioritized CAR for validation
74 because of its reported roles in protecting hepatocytes from drug- and BA-induced toxicity[8], which
75 include promoting hepatic MDR1 expression[9]. Individual shRNAmir expression experiments confirmed
76 that 3 of the 5 shRNAmirs against CAR reduced MDR1-dependent Rh123 efflux in Teff cells recovered
77 from transferred *Rag1*$^{-/-}$ mice (**Fig. 1c**, Extended Data Fig. 1c-d). These same three constructs diminished
78 MDR1 (*Abcb1a*) and CAR (*Nr1i3*) gene expression, as judged by qPCR, as well as expression of the
79 signature CAR transcriptional target gene, *Cyp2b10*[10] (Extended Data Fig. 1e).
80 CAR binds to DNA and regulates transcription as a heterodimer with retinoid X receptors
81 (RXRα/β/γ)[11]. However, RXRs also dimerize with many other NRs, including retinoic acid receptors
82 (RARα/β/γ), peroxisome proliferator-activated receptors (PPARα/δ/γ) and vitamin D receptor (VDR),
83 all of which regulate diverse aspects of T cell function *in vivo*. Consistent with this broader function of
84 RXRs, shRNAmir-mediated depletion of RXRα—the major RXR isoform expressed in T cells—did not
85 selectively regulate MDR1 expression in mucosal T cells, but rather impaired the persistence of
86 circulating Teff cells (Extended Data Fig. 1f). Depletion of the CAR-related xenobiotic-sensor, pregnane
87 X receptor (PXR)[12], influenced neither mucosal MDR1 expression nor Teff cell persistence *in vivo* (**Fig.
88 1b**; Extended Data Fig. 1f). In line with this result, Teff cells from C57BL/6 (B6)-derived CAR-deficient
89 (*Nr1i3*$^{-/-}$) mice displayed lower MDR1 expression and function than those from PXR-deficient (*Nr1i2*$^{-/-}$
90) mice, after co-transfer into *Rag1*$^{-/-}$ mice together with CD45.1 wild type cells; Teff cells lacking both
91 CAR and PXR showed equivalently low MDR1 expression and function as those lacking only CAR
92 (Extended Data Fig. 1g-i). These data implicate CAR in the regulation of mucosal T cell function *in
93 vivo*.
94 shRNAmir-mediated CAR depletion in FVB wild type T cells exacerbated T cell transfer-
95 induced weight loss in *Rag1*$^{-/-}$ mice, and did so in a manner that correlated directly with the degree of
96 MDR1 down-regulation in these cells (**Fig. 1d-e**; Extended data Fig. 1c-d). This result was consistent

97 with our prior studies showing that transfer of FVB T cells lacking MDR1 (*Abcb1a*$^{-/-}$*Abcb1b*$^{-/-}$) into
98 syngeneic *Rag1*$^{-/-}$ mice produces more severe weight loss than that of wild type counterparts—due to
99 induction of both colitis and BA-driven ileitis[4]—and is distinct from wild type naïve CD4^{+} T cells, which
100 induce only colitis in immunodeficient hosts[13]. Naive T cells from B6-derived CAR-null (*Nr1i3*$^{-/}$) mice
101 also precipitated more severe weight loss and ileitis, but equivalent colitis, compared with wild type
102 counterparts, after transfer into *Rag2*$^{-/-}$ mice that were co-housed to normalize microflora (**Fig. 1f-h**).
103 Therapeutic administration of the BA sequestering resin, cholestyramine (CME)[14], which binds BAs in
104 the lumen of the small intestine and prevents reabsorption into the ileal mucosa, normalized weight loss
105 and ileitis between *Rag2*$^{-/-}$ mice receiving CAR-sufficient or CAR-deficient T cells (Extended Data Fig.
106 2a-b); as did ablation of the ileal BA reuptake transporter, Apical sodium-dependent BA transporter
107 (Asbt/*Slc10a2*)[15] in *Rag1*$^{-/-}$ T cell recipients (Extended Data Fig. 2c-d). Neither genetic nor
108 pharmacological inhibition of ileal BA reabsorption affected the severity of T cell transfer-induced
109 colitis (Extended Data Fig. 2b, 2d). These results suggest that CAR acts in T cells selectively to promote
110 small bowel immune homeostasis, and that loss of CAR in T cells exacerbates ileitis that is not
111 transmissible by microbiota and requires BA reabsorption.

112 To elucidate CAR-dependent transcriptional programs in mucosal T cells, we used RNA-seq to
113 analyze the transcriptomes of wild type and CAR-deficient Teff cells from spleen, siLP and colon lamina
114 propria (cLP) of congenically co-transferred *Rag1*$^{-/-}$ mice—where CD45.1 CAR-sufficient and CD45.2
115 CAR-deficient Teff cells were present as tissue bystanders in the same animals (**Fig. 2a**). Wild type Teff
116 cell gene expression differed substantially in spleen, siLP and cLP, whereas CAR-deficiency most
117 conspicuously altered T cell gene expression in siLP (**Fig. 2b**). siLP Teff cells lacking CAR failed to
118 upregulate dozens of 'siLP-signature' genes (*i.e.*, genes increased in wild type siLP Teff cells, compared
119 to those from either spleen or colon), and acquired transcriptional features of wild type Teff cells from
120 the colon (**Fig. 2c-d**). CAR-dependent siLP-signature genes included chaperones, receptors and enzymes
121 involved in lipid binding, transport and metabolism (*e.g.*, *Apold1*, *Pex26*, *Dgkh*, *Ldlr*, *Phyhd1*, *Lclat1*;
122 **Fig. 2c**), and were enriched for genes previously found to be induced by CAR in mouse hepatocytes, by
123 RNA-seq, after *in vivo* administration of the synthetic CAR agonist ligand, 1,4-*Bis*(3,5-Dichloro-2-
124 pyridinyloxy) benzene (TCPOBOP, or simply TC)[16] (Extended Data Fig. 3a-b). Genes displaying CAR-
125 dependent expression in both siLP Teff cells and hepatocytes were enriched for loci at which TC-
126 inducible binding of a GFP-tagged mouse CAR protein was previously determined in hepatocytes by
127 ChIP-seq[17] (Extended Data Fig. 3c). As expected, these presumed CAR target genes included
128 MDR1/*Abcb1a* and *Cyp2b10*, but also other ABC-family transporters (*e.g.*, *Abcb4*) and cytochrome
129 P450 enzymes (*e.g.*, *Cyp2r1*) (Extended Data Fig. 3d), consistent with induction of a BA detoxification

program. CAR-deficient Teff cells showed reduced persistence in reconstituted *Rag1*$^{-/-}$ mice, relative to co-transferred CD45.1 wild type cells; this was most pronounced in siLP (Extended Data Fig. 4a-c), and trended towards being rescued by ablation of Asbt-dependent BA reabsorption in *Rag1*$^{-/-}$ recipients (Extended Data Fig. 4d-f).

Preferential CAR activity in mouse siLP Teff cells suggested that CAR might also regulate human T cell function in the small intestine. Therefore, we analyzed the expression and function of CAR in human peripheral blood T cell subsets expressing the small bowel-homing receptors, α4β7 integrin and CCR9[18], which are more likely to have recently recirculated from the intestinal mucosa. A small but reliable subset of α4^{+}β7^{+}CCR9^{+} Teff cells (~ 1-5%) was detected in peripheral blood of healthy adult donors (Extended Data Fig. 5a-c). Expression of these receptors was absent on naïve CD4^{+} T cells, as expected, and reduced among circulating CD25^{+} T regulatory (Treg) cells (Extended Data Fig. 5a-c), suggesting that Treg cells may be more efficiently retained in the intestinal mucosa than Teff cells. Given the lack of specific CAR antibodies, we assessed CAR expression and function based on predicted transcriptional outputs, beginning with MDR1. MDR1-dependent Rh123 efflux was undetectable in circulating CD4^{+} naïve and Treg cells, but increased progressively as human Teff cells acquired expression of α4 integrin, β7 integrin, and CCR9 (Extended Data Fig. 5d-e). α4^{+}β7^{+}CCR9^{+} Teff cells also displayed increased *ex vivo* expression of *ABCB1*, as judged by qPCR, as well as of CAR (*NR1I3*) and *CYP2B6*—the human ortholog of mouse *Cyp2b10* and hallmark CAR transcriptional target[19]—compared with naïve, Treg or α4^{-}β7^{-}CCR9^{-} Teff cells (Extended Data Fig. 5f). Most importantly, only α4^{+}β7^{+}CCR9^{+} Teff cells responded to *ex vivo* treatment with the human CAR agonist ligand, 6-(4-Chlorophenyl)imidazo[2,1-b][1,3]thiazole-5-carbaldehyde O-(3,4-dichlorobenzyl) oxime (CITCO)[19] by upregulating *CYP2B6* and *ABCB1* (Extended Data Fig. 5g-h). α4^{+}β7^{+}CCR9^{+} Teff cells were enriched for CCR6^{+}CXCR3^{hi}CCR4^{lo} "Th17.1" cells (Extended Data Fig. 5i-l), which display both Th17 and Th1 effector functions, as well as elevated MDR1 expression[20]. Nonetheless, combined expression of α4 integrin, β7 integrin, and CCR9 increased the proportion of MDR1-expressing Th17.1 cells, as well as of MDR1-expressing Th17 (CCR6^{+}CXCR3^{lo}CCR4^{hi}) and Th1 (CCR6^{-}CXCR3^{hi}CCR4^{lo}) cells, compared with lineage counterparts lacking one or more small bowel-homing receptors (Extended Data Fig. 5m-n). These data suggest that CAR is preferentially active in both mouse and human small intestinal Teff cells.

Enhanced CAR function in siLP Teff cells could involve local activation by endogenous metabolites. Consistent with this possibility, bile (from gallbladder), as well as sterile, soluble small intestine lumen content (siLC) from wild type B6 mice—but not colon lumen content (cLC) or serum—

162 induced *Abcb1a* and *Cyp2b10* upregulation in *ex vivo*-stimulated wild type, but not CAR-deficient, Teff
163 cells from spleens of reconstituted *Rag1*$^{-/-}$ mice (**Fig. 2e**; Extended Data Fig. 6a). CAR-dependent gene
164 expression in this *ex vivo* culture system was also induced by TC, inhibited by the CAR inverse agonist,
165 5α-Androstan-3β-ol[8], and unaffected by the PXR agonist, 5-Pregnen-3β-ol-20-one-16α-carbonitrile
166 (PCN)[12] (**Fig. 2e**; Extended Data Fig. 6a). The same dilutions of bile and siLC that enhanced CAR-
167 dependent gene expression in Teff cells also promoted recruitment of a co-activator peptide (PGC1α) to
168 recombinant CAR-RXRα ligand-binding domain (LBD) heterodimers, but not to RXRα LBD
169 homodimers, in time-resolved fluorescence resonance energy transfer (TR-FRET) experiments (**Fig. 2f-**
170 **g**; Extended Data Fig. 7a-b). Since CAR is thought to indirectly sense, but not directly bind, major BA
171 species[21], these data suggested that components of bile other than BAs might activate the CAR LBD;
172 bile consists of mixed micelles containing BAs, phospholipids, cholesterol, fatty acids and bile pigments
173 (*e.g.*, bilirubin)[1]. Consistent with a BA-independent mechanism of CAR activation, siLC-mediated
174 CAR-RXRα LBD heterodimer activation was not affected by CME-mediated depletion of free BAs
175 (Extended Data Fig. 7c), and no major primary or secondary BA species was sufficient to activate CAR-
176 RXRα LBD heterodimers in TR-FRET experiments, or to stimulate CAR-dependent gene expression in
177 *ex vivo*-cultured Teff cells (Extended Data Fig. 7d, data not shown). CAR-RXRα LBD heterodimers
178 were also activated by siLC from germ-free (GF) wild type mice (Extended Data Fig. 7c, data not
179 shown). Thus, host-derived, non-BA constituents of bile may directly enhance CAR transcriptional
180 activity in siLP Teff cells.

181 To further explore CAR immunoregulatory functions, we used gene set enrichment analysis
182 (GSEA) to examine the impact of CAR-deficiency on gene expression previously associated with major
183 pro- and anti-inflammatory T helper cell lineages. Unexpectedly, siLP Teff cells lacking CAR displayed
184 reduced gene expression ascribed to type 1 regulatory (Tr1) cells[22], a key subset of Foxp3^{-}IL-10^{+} T cells
185 recognized for suppressing mucosal inflammation in humans and mice (**Fig. 3a-c**)[23]. Consistent with
186 this, CAR was strictly required for the expression of both a Thy1.1-expressing *Il10*-reporter allele[24]
187 (10BiT; **Fig. 3d-e**) and endogenous IL-10 protein (Extended Data Fig. 8a-e) in Teff cells re-isolated
188 from transferred *Rag1*$^{-/-}$ mice. Conversely, TC, as well as bile and siLC from wild type mice, induced
189 CAR-dependent *Il10* upregulation in *ex vivo*-stimulated Teff cells (**Fig. 3f**; Extended Data Fig. 6), akin
190 to *Abcb1a* and *Cyp2b10* (**Fig. 2e**). Colon lumen content acted on both wild type and CAR-deficient Teff
191 cells to enhance *Il10* expression (**Fig. 3f**), suggesting that non-overlapping CAR-dependent and CAR-
192 independent pathways may modulate *Il10* expression in mucosal T cells in the small and large intestines,
193 respectively. CAR-dependent IL-10 expression in the *Rag1*$^{-/-}$ T cell transfer model was transient—

194 peaking 2-weeks after T cell engraftment and waning thereafter—and followed the kinetics of both T
195 cell infiltration into siLP and *ex vivo* CAR (*Nr1i3*), MDR1 (*Abcb1a*) and *Cyp2b10* gene expression
196 (Extended Data Fig. 8f-h). CAR was also required for IL-10 expression in endogenous siLP effector and
197 regulatory T cell subsets from intact mice, but only after injection of soluble anti-CD3 antibodies to
198 induce acute intestinal inflammation[23] (Extended data Figure 9a-c). In addition, CAR/*Nr1i3* expression
199 was upregulated during the *in vitro* development of Tr1 cells, where naïve $CD4^+$ T cells were activated
200 and expanded in the combined presence of IL-27—a cytokine that promotes Stat3-dependent IL-10
201 expression[22]—and the synthetic corticosteroid, dexamethasone[25] (**Fig. 3g**). Loss of CAR restricted IL-
202 10 production by these *in vitro*-polarized Tr1 cells (**Fig. 3h-i**). By contrast, CAR expression was not
203 induced during the *in vitro* development of other conventional effector (*e.g.*, Th1, Th2, Th17) or
204 regulatory (*e.g.*, induced (i)Treg) lineages, compared with naïve T cells, and loss of CAR had no bearing
205 on the *in vitro* development of these cells (**Fig. 3g**, Supplemental Table 2). These data reveal a novel and
206 essential function for CAR in *Il10* gene regulation, whether direct or indirect, which may synergize with
207 the CAR-dependent BA detoxification program in mucosal T cells to foster resolution of small bowel
208 inflammation.

209 Gene expression associated with Th17 cells—an important lineage of $ROR\gamma t^+$ pro-inflammatory
210 T cells implicated in the pathogenesis of inflammatory bowel diseases[26]—was reciprocally increased in
211 siLP Teff cells lacking CAR (**Fig. 3b**), and reduced IL-10 expression in Teff cells lacking CAR
212 paralleled their accumulation as $ROR\gamma t^+$IL-17A$^-$ 'poised' Th17 cells[27,28] in siLP of transferred *Rag1*$^{-/-}$
213 mice (Extended Data Fig. 9d-e). However, this phenotype was recapitulated by *Il10*$^{-/-}$ Teff cells replete
214 for CAR (Extended Data Fig. 9f-g), suggesting that CAR might suppress the development and/or
215 accumulation of mucosal Th17 cells indirectly, via IL-10 induction. Other effector and regulatory T cell
216 gene signatures were unaffected by loss of CAR *in vivo* (**Fig. 3b**).

217 Finally, we reasoned that if CAR-deficiency in Teff cells exacerbates BA-driven small bowel
218 inflammation, pharmacologic CAR activation might be protective. A single administration of the
219 selective CAR agonist, TC, to *Rag1*$^{-/-}$ mice reconstituted with a mixture of CD45.1 wild type and CD45.2
220 CAR-deficient T cells was sufficient to induce *Abcb1a*, *Cyp2b10* and *Il10* upregulation in wild type, but
221 not CAR-deficient, Teff cells within 72 hr (**Fig. 4a**). Weekly TC administration reduced ileitis, but not
222 colitis, in *Rag2*$^{-/-}$ mice reconstituted with only wild type T cells and fed a standard 0.2% cholic acid
223 (CA)-supplemented diet to increase the size of the circulating BA pool and promote small bowel injury[28]
224 (**Fig. 4b-c**); CA-feeding increased morbidity and mortality in *Rag2*$^{-/-}$ mice receiving wild type T cells,
225 but had no obvious effects on *Rag2*$^{-/-}$ mice in the absence of T cell transfer (**Fig. 4b**, data not shown). As

226 expected, therapeutic effects of TC were abolished in CA-fed *Rag2*$^{-/-}$ mice reconstituted with CAR-
227 deficient T cells (Extended Data Fig. 10). These data suggest that BA-supplementation promotes,
228 whereas CAR activation in T cells suppresses, experimental ileitis. Although additional effects of TC-
229 mediated CAR activation in parenchymal tissues could not be discerned from these studies, the results
230 reveal an unexpected new strategy for the treatment of small bowel Crohn's disease.

231 BAs have emerged as important and pleotropic signaling metabolites that have both pro- and
232 anti-inflammatory effects in the gastrointestinal tract via dynamic interactions with germline-encoded
233 host receptors and the microbiota[1]. Whereas low (micromolar) concentrations of secondary BAs in the
234 colon—produced via bacterial metabolism—appear to support mucosal immune tolerance by activating
235 and expanding colonic Foxp3^{+} Treg cells[29,30], the higher (millimolar) concentrations of primary BAs
236 present in the small intestine—due to active reuptake during enterohepatic circulation—may be more
237 pro-inflammatory and cytotoxic. Our study suggests that the BA- and xenobiotic-sensing nuclear
238 receptor, CAR/Nr1i3, reprograms mucosal T cell gene expression in the small intestine to counter BA-
239 induced toxicity and inflammation (**Fig. 4d**). The additional contribution of non-BA components in bile
240 to CAR activation in small intestinal T cells suggests more direct, extensive and compartmentalized
241 interplay between mucosal T cells and hepatic metabolism than previously recognized. Pharmacologic
242 CAR activation not only offers a new and more targeted approach to treat small bowel Crohn's disease;
243 it also opens new avenues for exploring lymphocyte specialization across the intestinal tract.
244
245

246 Experimental procedures

247

248 Mice

249 C57BL/6 (B6)-derived wild type (Stock No: 000664), CD45.1 (Stock No: 002014), *Rag1*$^{-/-}$ (Stock
250 No: 002216), *Rag2*$^{-/-}$ (Stock No: 008449) and *Il10*$^{-/-}$ (Stock No: 004368) mice were purchased from The
251 Jackson Laboratory. Wild type FVB/N mice were purchased from Taconic. B6-derived *Nr1i2*$^{-/-}$, *Nr1i3*$^{-}$
252 $^{/-}$ and *Nri12*$^{-/-}$*Nr1i3*$^{-/-}$ mice were provided by D. Moore (Baylor College of Medicine, BCM). FVB-
253 derived *Rag1*$^{-/-}$ mice were a gift of Dr. Allan Bieber (Mayo Clinic, Rochester, MN). B6-derived BAC
254 *Il10*-Thy1.1 transgenic reporter (10BiT) mice were provided by C. Weaver (University of Alabama-
255 Birmingham, UAB) and have been described previously[24]. B6-derived *Rag1*$^{-/-}$ mice were crossed with
256 *Slc10a2*$^{-/-}$ mice (gift of Dr. Paul Dawson, Emory University) in the Sundrud lab to generate *Rag1*$^{-/-}$ mice
257 lacking the Asbt transporter as in[4]. Lumen contents (colon, small intestine) were harvested (see below)

258 from specific pathogen-free (SPF) or germ-free wild type B6 mice housed at the University of Alabama-
259 Birmingham (UAB; courtesy of Dr. Weaver). All breeding and experimental use of animals was
260 conducted in accordance with protocols approved by IACUC committees at Scripps Florida, BCM or
261 UAB.
262
263 **Human blood samples**
264 Human blood samples were collected and analyzed in accordance with protocols approved by
265 Institutional Review Boards at Scripps Florida and OneBlood (Orlando, Florida). Blood was obtained
266 following informed written consent, and consenting volunteers willingly shared clinical history and
267 demographic information prior to phlebotomy. Institutional Review Boards at OneBlood and Scripps
268 Florida approved all procedures and forms used in obtaining informed consent, and all documentation
269 for consenting volunteers is stored at OneBlood.
270
271 **$CD4^+$ T cell isolation and culture**
272 Purified $CD4^+CD25^-$ T cells were magnetically isolated from spleen and peripheral lymph node
273 mononuclear cells using an EasySep magnetic T cell negative isolation kit (Stem Cell Technologies,
274 Inc.) with addition of a biotin anti-mouse CD25 antibody (0.5 µg/mL; BioLegend). Magnetically-
275 enriched $CD4^+$ T cells were cultured in (DMEM) supplemented with 10% heat-inactivated fetal bovine
276 serum, 2mM L-glutamine (Gibco), 50uM 2-mercaptoethanol (Amresco), 1% MEM vitamin solution
277 (Gibco), 1% MEM non-essential amino acids solution(Gibco), 1% Sodium Pyruvate(Gibco), 1%
278 Arg/Asp/Folic acid (Gibco), 1% HEPES (Gibco), 0.1% gentamicin (Gibco) and 100u/ml Pen-Strep
279 (Gibco). For *Rag1*$^{-/-}$ transfer experiments, magnetically enriched $CD4^+CD25^-$ T cells were FACS-sorted
280 to obtain pure naïve T cells ($CD3^+CD4^+CD25^-CD62L^{hi}CD44^{lo}$). For *ex vivo* isolation of mononuclear
281 cells from tissues of T cell-reconstituted Rag-deficient mice, single cell suspensions were prepared from
282 spleen, peripheral lymph nodes, or mesenteric lymph nodes (MLN) by mechanical disruption passing
283 through 70 µm nylon filters (BD Biosciences). For intestinal tissues, small intestines and colons were
284 removed, rinsed thoroughly with PBS to remove the fecal contents, and opened longitudinally; Peyer's
285 patches were removed from small intestines. Tissues were incubated for 30 minutes at room temperature
286 in DMEM media without phenol red (Genesee Scientific) plus 0.15% DTT (Sigma-Aldrich) to eliminate
287 mucus layer. After washing with media, intestines were incubated for 30 minutes at room temperature
288 in media containing 1 mM EDTA (Amresco) to remove the epithelium. Intestinal tissue was digested in
289 media containing 0.25 mg/mL liberase TL (Roche) and 10 U/mL RNase-free DNaseI (Roche) for 15-25

290 minutes at 37 ºC. Lymphocyte fractions were obtained by 70/30% Percoll density gradient centrifugation
291 (Sigma-Aldrich). Mononuclear cells were washed in complete T cell media and resuspended for
292 downstream FACS analysis or sorting.
293 *Naïve CD4$^+$ T cell activation and polarization*: magnetically enriched CD4$^+$CD25$^-$ T cells were seeded
294 (at 4x10^5 cells/cm^2 and 1x10^6 cells/mL) in 96- or 24-well flat bottom plates pre-coated for 1-2 hr at 37
295 ºC with goat-anti-hamster whole IgG (50 μg/mL; Invitrogen). Activation was induced by adding
296 hamster-anti-mouse CD3ε (0.3 or 1 μg/mL; BioLegend) and hamster-anti-mouse CD28 (0.25 or 0.5
297 μg/mL; BioXcell). After 48 hr, cells were removed from coated wells and re-cultured at 1x10^6 cells/mL
298 in media with or without 10 U/mL recombinant human IL-2 (rhIL-2) (NIH Biorepository), depending
299 on the experiment (see below). For polarization studies, cells were activated in the presence of the
300 following sets of cytokines and/or neutralizing antibodies (all from R&D Systems): Th0—media alone;
301 Th1—recombinant human (rh)IL-12 (5 ng/mL) plus anti-mouse IL-4 (5 μg/mL); Th2—rhIL-4 (10
302 ng/mL) plus anti-mouse IFNγ (5 μg/mL); non-pathogenic (np)Th17—recombinant mouse (rm)IL-6 (40
303 ng/mL) plus rhTGFβ1 (1 ng/mL), anti-mouse IFNγ (5 μg/mL) and anti-mouse IL-4 (5 μg/mL);
304 pathogenic (p)Th17— rmIL-6 (40 ng/mL) plus rhTGFβ1 (1 ng/mL), rhIL-23 (10 ng/mL) anti-mouse
305 IFNγ (5 μg/mL) and anti-mouse IL-4 (5 μg/mL); induced T regulatory (i)Treg—rhTGFβ1 (5 ng/mL)
306 plus rhIL-2 (10 U/mL), anti-mouse IFNγ (5 μg/mL) and anti-mouse IL-4 (5 μg/mL). For Tr1 cultures,
307 cells were activated in the presence of rhIL-27 (100 ng/mL) and/or dexamethasone (100 nM; Sigma-
308 Aldrich). Cytokine, antibodies and/or Dex were added at the time of activation (day 0), and re-added to
309 expansion media between days 2-4 of culture. Cells were analyzed for intracellular expression of
310 transcription factors and/or cytokines, to confirm polarization, on day 4 after re-stimulation with phorbol
311 12-myrisate 13-acetate (PMA; 10nM; Life Technologies) and ionomycin (1uM; Sigma-Aldrich) for 3-4
312 hr in the presence of brefeldin A (BFA; 10ug/mL; Life Technologies).
313 *Ex vivo-stimulation of FACS-sorted effector/memory (Teff) cells from reconstituted Rag1$^{-/-}$ mice*: 30,000
314 CD45.1 (wild type) or CD45.2 (*Nr1i3$^{-/-}$*) cells—FACS-purified from spleens of B6.*Rag1$^{-/-}$* 2-3 weeks
315 post naïve T cell transfer—were activated in round-bottom 96-well plates with mouse anti-CD3/anti-
316 CD28 T cell expander beads (1 bead/cell; Life Technologies) in complete media containing 10 U/mL
317 recombinant human (rh) IL-2 for 24 hr in the presence or absence of synthetic or endogenous CAR
318 agonists (see 'compound and tissue extracts' below).
319
320 **Retroviral plasmids and transductions**

321 shRNAmirs against mouse nuclear receptors were purchased (TransOMIC) or custom synthesized using
322 the shERWOOD algorithm[41]. For cloning into an ametrine-expressing murine retroviral vector (LMPd)
323 containing the enhanced miR-30 cassette[42,43], shRNAmirs were PCR amplified using forward (5′-
324 AGAAGGCTCGAGAAGGTATATTGC-3′) and reverse (5′-GCTCGAATTCTAGCCCCTTGAAGTC
325 CGAGG-3′) primers containing XhoI and EcoR1 restriction sites, respectively. All retroviral constructs
326 were confirmed by sequencing prior to use in cell culture experiments. Retroviral particles were
327 produced by transfection of Platinum E (PLAT-E) cells with the TransIT-LT1 transfection reagent
328 (Mirus) in Opti-MEM I reduced serum medium. Viral supernatants containing 10 µg/mL polybrene were
329 used to transduce $CD4^{+}CD25^{-}$ T cells 24 hr post-activation (anti-CD3/anti-CD28; as above).
330 Transductions were enhanced by centrifugation at 2000 rpm for 1 hr at room temperature, and incubation
331 at 37 ºC until 48 hr post-activation. Transduced cells were expanded in complete media containing 10
332 U/mL rhIL-2.
333
334 **Cell lines**
335 PLAT-E cells, derived from the HEK-293 human embryonic kidney fibroblasts and engineered for
336 improved retroviral packaging efficiency, were provided by M. Pipkin (Scripps Florida). All cell lines
337 were tested to be mycoplasma free, and cultured in DMEM plus 10% FBS, 2 mM L-glutamine, 50 uM
338 2-mercaptoethanol, 1% HEPES, 0.1% gentamicin and 100u/ml Pen-Strep.
339
340 **T cell transfer colitis**
341 For experiments using B6-derived wild-type or CAR-deficient (*Nr1i3*$^{-/-}$) T cells, 0.5 x 10^6 FACS-sorted
342 naïve T cells (sorted as $CD4^{+}CD25^{-}CD62L^{hi}CD44^{lo}$ at Scripps Florida; $CD4^{+}CD45RB^{hi}$ at BCM) were
343 injected intraperitoneally (i.p.) into syngeneic *Rag1*$^{-/-}$ (at Scripps Florida) or *Rag2*$^{-/-}$ (at BCM) recipients
344 and analyzed between 2-6 weeks post-transfer. For mixed congenic T cell transfers, FACS-purified naïve
345 T cells ($CD4^{+}CD25^{-}CD62L^{hi}CD44^{lo}$) from CD45.1 wild type and CD45.2 CAR-deficient (*Nr1i3*$^{-/-}$),
346 PXR-deficient (*Nr1i2*$^{-/-}$), CAR- and PXR-deficient (*Nri12*$^{-/-}$*Nr1i3*$^{-/-}$) or *Il10*$^{-/-}$ mice were mixed in a 1:1:
347 ratio and transferred together (0.5 x 10^6 total cells). For transfers of shRNAmir-expressing T cells,
348 magnetically enriched $CD4^{+}CD25^{-}$ T cells from FVB/N (FVB) wild-type mice, activated and transduced
349 as above, were expanded until day 5 in media containing rhIL-2 and transferred into syngeneic *Rag1*$^{-/-}$
350 mice (0.5 x 10^6 total cells). All *Rag1*$^{-/-}$ recipients were weighed immediately prior to T cell transfer to
351 determine baseline weight, and then weighed twice weekly after T cell transfer for the duration of the
352 experiment. Mouse chow diets containing 2% Cholestyramine (CME) (Sigma-Aldrich) or 0.2% Cholic

353 Acid (CA) (Sigma-Aldrich) and control diets were custom made (Teklad Envigo, Madison, WI) and fed
354 to mice as follows: CME-supplemented diets were started 3 weeks after T cell transfer and continued for
355 3 weeks; cholic acid diet was started within 3 days post-T cell transfer and continued for 6 weeks (or
356 until mice died). TCPOBOP (TC; Sigma-Aldrich) was initially reconstituted in sterile DMSO, stored at
357 -20 ºC, and diluted in sterile saline and sonicated immediately prior to injections. 3 mg/kg TC was
358 injected intra-peritoneal (i.p.) weekly as indicated. Transferred *Rag1*$^{-/-}$ or *Rag2*$^{-/-}$ mice were euthanized
359 upon losing 20% of pre-transfer baseline weight. All *Rag*$^{-/-}$ mice receiving different donor T cell
360 genotypes were co-housed to normalize microflora exposure.
361
362 **Anti-CD3-induced intestinal injury**
363 Wild-type (B6) or CAR-deficient (B6.*Nr1i3*$^{-/-}$) mice were injected i.p. with 15 ug of soluble, Ultra-LEAF
364 purified anti-CD3 (clone: 145-2C11) or IgG isotype control (clone: HTK888) (BioLegend) twice over
365 48 hr. Animals were euthanized, and T cells analyzed 4 hr after the second injection.
366
367 **Histology**
368 Colon (proximal, distal) or small intestine (proximal, mid, distal/ileum) sections (~ 1 cm) were cut from
369 euthanized *Rag1*$^{-/-}$ or *Rag2*$^{-/-}$ mice 6 weeks post-T cell transfer. In some experiments, 10 cm segments
370 of distal small intestine and whole colon were dissected from mice and fixed intact. All tissues were
371 fixed in 10% neutral buffered formalin, embedded into paraffin blocks, cut for slides at 4-5 microns, and
372 stained with hematoxylin and eosin (H&E). H&E-stained sections were analyzed and scored blindly by
373 a pathologist with GI expertise using an Olympus BX41 microscope and imaged using an Olympus
374 DP71 camera. Colons and ilea were histologically graded for inflammation severity using a combination
375 of previously-reported grading models published by Kim, et al.[31] and by Berg et al.[32]. The scheme
376 published by Kim, et al grades 5 different descriptors which include crypt architecture (normal, 0 - severe
377 crypt distortion with loss of entire crypts, 3), degree of inflammatory cell infiltration (normal, 0 – dense
378 inflammatory infiltrate, 3), muscle thickening (base of crypt sits on the muscularis mucosae, 0 - marked
379 muscle thickening present, 3), goblet cell depletion (absent, 0- present, 1) and crypt abscess (absent, 0-
380 present, 1). Berg et al uses a grade 0 through 4 model of overall severity with grade 1 being normal and
381 grade 4 showing diffuse intestinal involvement with transmural inflammation, marked epithelial
382 hyperplasia, marked mucin depletion with abscesses and ulcers.
383
384 **Flow cytometry**

385 Cell surface and intracellular FACS stains were performed at 4 ºC for 30 minutes, washed with phosphate
386 buffered saline (PBS) and acquired on a flow cytometer. Analysis of Rh123 efflux was performed as in[4].
387 Background Rh123 efflux was determined by the addition of the MDR1 antagonist, elacridar (10 nM),
388 to Rh123-labelled cells prior to the 37 ºC efflux step. Anti-mouse antibodies used for FACS analysis
389 included: Alexa Fluor 700 anti-CD45, APC anti-CD45.1, BV711 anti-CD4, BV510 anti-CD25, BV650
390 anti-CD3, Percp-Cy5.5 anti-CD62L, PE-CY7 anti-CD44, BV605 anti-CD62L, PE anti-α4β7, Alexa
391 Fluor700 anti-CD4, FITC anti-CD44, BV421 anti-CD44, e450 anti FOXP3, BV605 anti-TNF, Percp-
392 Cy5.5 anti-Il-17a, BV711 anti-INFγ, PE anti-Il-4, PE-CY7 anti-IL-10, PE anti-Thy1.1, FITC anti-CD3,
393 Percp-Cy5.5 anti-Thy1.1, PE anti-CD3, PE anti-TCRβ, APC anti-INFg, FITC anti-CD45.2, PE anti-
394 α4β7 (from BioLegend); and BUV395 anti-CD3, PE-CF594 anti-CD25, FITC anti-Ki-67, PE-CF594
395 anti-RORγt (from BD). Anti-human antibodies used for FACS analysis included: APC anti-CD3, PE
396 anti-CD4, PE-Cy7 anti-CD45RO, BV711 anti-CD49a (integrin α4), APC-Fire 750 anti-integrin β7,
397 BV421 anti-CCR9, and Percp-Cy5.5 anti-CCR7, BV605 anti-CCR2, PE anti-CRTH2, PE anti-CCR10,
398 PE-Cy7 anti-CCR4, Percp-Cy5.5 anti-CXCR3, APC anti-CCR6, BV605 anti-CD4, PE-CF594 anti-
399 CD25 (from BD). Vital dyes include: fixable viability eFluor® 506, eFluor® 660 and eFluor® 780 (all
400 from eBioscience). Rh123 and elacridar were purchased from Sigma-Aldrich. All FACS data was
401 acquired on LSRII or FACSCanto II instruments (BD), and analyzed using FlowJo 9 or FlowJo 10
402 software (TreeStar, Inc.). (We're probably missing a bunch).
403
404 **FACS sorting**
405 Cells stained with cell-surface antibodies, as above, were passed through 70 μm nylon filters,
406 resuspended in PBS plus 1% serum, and sorted on a FACS AriaII machine (BD Biosciences). Sorted
407 cells were collected in serum-coated tubes containing PBS plus 50% serum. Gates used to sort MDR1+/-
408 T cells, based on Rh123 efflux, were set using background Rh123 efflux in elacridar-treated cells. For
409 human T cell sorts, Peripheral blood mononuclear cells (PBMC) were isolated using Ficoll-Plaque PLUS
410 (GE Healthcare) from 25 mL of enriched buffy coats (OneBlood). $CD4^+$ T cells were enriched using the
411 Human total CD4 T cell Negative Isolation kit (EasySep), followed by enrichment of either
412 effector/memory T cells (Human Memory CD4 T cell Enrichment kit; EasySep) or Treg cells (Human
413 $CD4^+CD127^{lo}CD49d^-$ Treg Enrichment Kit; EasySep) (all from StemCell Technologies). Enriched cells
414 were stained with anti-human FACS antibodies (listed above) for 20 minutes on ice. Stained cells were
415 filtered through sterile 40 uM mesh filters and re-suspended in PBS with 5% FBS and 0.1% DNase. In
416 cases where RNA was isolated after sorting, 100,000 cells were sorted into 200 uL PBS with 1 uM DTT

417 and 5 uL RNase Inhibitor Cocktail (Takara); for *ex vivo* culture experiments, 0.4-1.2 x10^6 cells were
418 sorted into complete T cell media.
419
420 **Pooled *in vivo* shRNAmir screen**
421 Two independent pooled screens were performed. Briefly, PLAT-E cells were cultured in 96 well plates
422 with 5 x 10^4 per well in 100uL complete medium and transfected as described above. Magnetically
423 enriched $CD4^+CD25^-$ T cells from spleens of 7- to 8-week old female FVB/N (FVB) mice were activated
424 with anti-CD3 and anti-CD28 in 96 well plates and transduced 24 hr post-activation. Transduction
425 efficiency of each individual shRNA was determined on day 4; transduced cells were pooled and FACS-
426 sorted for ametrine$^+$ on day 5 and adoptively transferred (i. p.) into 10 FVB.*Rag1*$^{-/-}$ mice. An aliquot of
427 sorted cells was saved for genomic DNA isolation and used for input reference. Six weeks post-transfer,
428 live (viability dye$^-$) transduced (ametrine$^+$) Rh123^{hi} (Mdr1$^-$) or Rh123^{lo} (Mdr1$^+$) effector/memory T cells
429 (Teff; $CD4^+CD25^-CD62L^{lo}CD44^{hi}$) were FACS-sorted from the spleen or small intestine lamina propria
430 of FVB.*Rag1*$^{-/-}$ recipients. High quality genomic DNA was isolated using PureLink® Genomic DNA
431 Mini Kit (Invitrogen) and 100 ng of DNA was used for library preparation. gDNA derived from
432 transduced and sorted T cells were quantified with Qubit DNA assay. 75ng of gDNA were used as
433 template in duplicate reactions to add the Ion adapter sequences and barcodes. Based on previous data,
434 28 cycles of PCRs were used to amplify the libraries using primers with Ion P1 miR30 loop sequence
435 (5'-CCTCTCTATGGGCAGTCGGTGATTACATCTGTGGCTTCACTA-3') and Ion A miR-30 (5'-
436 CCATCTCATCCCTGCGTGTCTCCGACTCAGXXXXXXXXXXGCTCGAGAAGGTATATTGCT-
437 3') sequences. The miR-30 loop (PI) and miR-30 (A) annealing sequences are underlined. The IonXpress
438 10 nt barcode is depicted with a string of X's. Sequencing libraries were purified with 1.6X Ampure XP
439 beads (Beckman Coulter), quantified with Qubit DNA HS assay (Invitrogen), and visualized on the
440 Agilent 2100 Bioanalyzer (Agilent Technologies, Inc.). Individually-barcoded libraries were pooled at
441 equimolar ratios and templated on to Ion spheres at 50 pM loading concentration using the Ion Chef
442 (Life Technologies) with the Ion PI IC 200 kit. The templated Ion spheres (ISPs) were quantified using
443 AlexaFluor sequence-specific probes provided in the Ion Spehere quality control kit (Life Technologies).
444 The percent templated ISPs within 10-20% were taken forward to loading on the Ion PI V2 chips and
445 then run on the Ion Proton with 200 bp reads. Libraries were sequenced using the Ion Torrent technology
446 from Life Technologies following the manufacturer's instructions. Sequencing reads were aligned to the
447 reference library using BLAST with default settings and raw counts were normalized with DESeq2.
448 Normalized reads of shRNAmirs displaying $\leq$ 10-fold change between input and *ex vivo* spleen samples
449 were considered for downstream analysis. The relative enrichment or depletion of shRNAmirs from each

450 population was determined by median log_2 fold-change in abundance of shRNAmirs in $Mdr1^{hi}$ *vs*. $Mdr1^{lo}$
451 siLP Teff cells.
452
453 **Compounds and tissue extracts**
454 10 or 20 uM 1,4-Bis-[2-(3,5-dichloropyridyloxy)]benzene, 3,3′,5,5′-Tetrachloro-1,4-bis(pyridyloxy)
455 benzene (TC), 10 uM 5α-Androstan-3β-ol (And), 10 uM 5-Pregnen-3β-ol-20-one-16α-carbonitrile
456 (PCN) (all from Sigma-Aldrich)—or serum, bile (from gallbladder), sterile soluble small intestine lumen
457 content (siLC), or sterile soluble colon lumen content (cLC) from wild type (B6) mice—were added to
458 mouse naïve or effector/memory (Teff) cells stimulated with anti-CD3/anti-CD28 antibodies as above.
459 For preparation of mouse tissue extracts, mouse small intestinal lumen content (siLC) or colon lumen
460 content (cLC) was extracted from whole tissue into a sterile tube. Contents were weighed, diluted with
461 an equal volume of sterile PBS, vortexed vigorously for 30 sec, and then supernatants were collected
462 after sequential centrifugation steps: (*i*) 10 min at 930 x *g*; and (*ii*) 10 min at 16 x *g*. Cleared supernatants
463 were finally sterile-filtered using 0.22 μm filters and aliquots were frozen at -20° C. Serum was collected
464 in EDTA coated tubes and centrifuged for 5 min at 2.4 x *g*. Due to small sample size, serum and
465 gallbladder bile were used directly without filter sterilization after harvesting. Equal volumes of sterile
466 vehicles (DMSO for TC, And; ethanol for PCN; PBS for sterile mouse content) served as negative
467 controls. For human T cell culture experiments, healthy adult donor PBMC were FACS-sorted for the
468 following subsets: (*i*) naïve $CD4^+$ T cells ($CD4^+CD25^-CD45RO^-CCR7^{hi}$); (*ii*) Treg cells ($CD4^+CD25^{hi}$);
469 (*iii*) $\alpha4^-CCR9^-$ effector/memory cells (Teff; $CD4^+CD25^-CD45RO^+$); and (*iv*) $\alpha4^+CCR9^+$
470 effector/memory cells (Teff; $CD4^+CD25^-CD45RO^+$). Note that all $\alpha4^-CCR9^-$ Teff cells are integrin $\beta7^-$
471 and all $\alpha4^+CCR9^+$ Teff cells are integrin $\beta7^+$. For all subsets, 30,000 purified cells were stimulated in
472 round-bottom 96-well plates with human anti-CD3/anti-CD28 T cell expander beads (1 bead/cell;
473 ThermoFisher) in complete media containing 10 U/mL rhIL-2 with or without 10 or 20 uM 6-(4-
474 Chlorophenyl)imidazo[2,1-b][1,3]thiazole-5-carbaldehyde O-(3,4-dichlorobenzyl)oxime (CITCO)
475 (Sigma-Aldrich); an equal volume of DMSO served as the negative control.
476
477 **qPCR**
478 RNA was isolated from cultured or ex vivo-isolated cells using RNeasy Mini columns with on-column
479 DNase treatment (Qiagen); RNA was used to synthesize cDNA via a high capacity cDNA reverse
480 transcription kit (Life Technologies). Taqman qPCR was performed on a StepOnePlus real time PCR
481 instrument (Life Technologies/Applied Biosystems) using commercial Taqman primer/probe sets (Life

482 Technologies). Probes for mouse genes included: *Abcb1a* (Mm00607939_s1), *Nr1i3*
483 (Mm01283981_g1), *Cyp2b10* (Mm01972453_s1), *Il10* (Mm01288386_m1) and *Actin b*
484 *(Mm00607939_s1)*; probes for human genes included: *NR1I3* (Hs00901571_m1), *ABCB1*
485 (Hs00184500_m1), *CYP2B6* (Hs04183483), *IL10* (Hs00961622_m1), and *ACTIN B* (Hs0160665_g1).
486

487 **Bioinformatics analyses**

488 *ChIP-seq*: Raw sequencing reads for CAR were downloaded from Gene Expression Omnibus
489 (GSE112199)[17], aligned to USC mm10 with Bowtie2[33] and analyzed with MACS[34] using base settings.
490 Biological replicate reads files were merged into a single file and bigwig files were generated and
491 visualized with Integrated Genome Viewer (IGV)[35]. Peaks were filtered to remove reads with alternative
492 annotations, mitochondrial DNA, or blacklist regions in R using GenomeInfoDb and GenomicRanges
493 package.

494 *RNA-seq*: Next-generation RNA-sequencing (RNA-seq) was performed on FACS-sorted B6 wild type
495 and CAR-deficient effector/memory T cells (Teff cells: viability dye^{-}CD45^{+}CD3^{+}CD4^{+}CD25^{-}CD44^{hi})
496 from spleen, small intestinal lamina propria, and colon lamina propria of *Rag1*$^{-/-}$ mice injected 3-weeks
497 prior with congenic mixtures of CD45.1 wild type and CD45.2 *Nr1i3*$^{-/-}$ naïve T cells, approximately 500
498 sorted cells were processed directly to generate cDNA using the Clontech SMART-Seq v4 Ultra Low
499 Input Kit (Clontech, Inc.) on three biologically-independent replicates. The generated cDNA was size
500 selected using beads to enrich for fragments > 400 bp. The enriched cDNA was converted to Illumina-
501 compatible libraries using the NEBNext Ultra II DNA kit (New England Biolabs, Inc.) using 1ng input.
502 Final libraries were validated on the Agilent 2100 bioanalyzer DNA chips and quantified on the Qubit
503 2.0 fluorometer (Invitrogen, Life Technologies). Barcoded libraries were pooled at equimolar ratios and
504 sequenced using single-end 75 bp reads on a NextSeq 500 instrument (Illumina). Raw sequencing reads
505 (fastq files) were mapped to the mm10 transcriptome and transcript abundance in terms of Transcripts
506 Per Million (TPM) were quantified using Salmon[48]. PCA was performed and projected in R-studio.
507 Differentially expressed genes (DEG) were determined using DESeq2 ($P < .05$) for CAR-deficient
508 (B6.*Nr1i3*$^{-/-}$) *vs.* wild type (B6) Teff cells from spleen (296 up; 285 down), siLP (472 up; 523 down), or
509 cLP (350 up; 228 down) and $\log_2$ fold-change was used as the ranking metric to generate input ranked
510 lists for gene set enrichment analysis (GSEA) (https://www.gsea-msigdb.org/gsea/index.jsp); these
511 genes were compared against both customized and curated gene sets (the latter from the Molecular
512 Signature Database (MSigDB)) for enrichment—quantified as normalized enrichment score (NES)—
513 and visualized using ggplot2 package in R. Differentially expressed genes of wild type (B6) Teff cells
514 from the spleen, siLP, or cLP determined by DESeq2 were used to generate tissue-specific Teff gene

515 sets: (*i*) up in B6 spleen Teff, genes selectively expressed in spleen *vs*. either siLP or cLP wild type (B6)
516 Teff cells; (*ii*) up in B6 siLP Teff, genes selectively expressed in siLP *vs*. either spleen or cLP wild type
517 (B6) Teff cells; and (*iii*) up in B6 cLP Teff, genes selectively expressed in cLP *vs*. either spleen or siLP
518 wild type (B6) Teff cells. RNA-seq data of pharmacological activation of CAR or PXR in hepatocytes
519 *in vivo* from mice treated with the CAR agonist, TCPOBOP (TC), the PXR agonist, PCN, or vehicle
520 (corn oil) (GSE104734)[16] were analyzed to generate the gene sets: Up in Hep + TC, genes selectively
521 induced by the CAR agonist, TCPOBOP (TC), compared with either vehicle (corn oil) or the PXR
522 agonist, PCN, in hepatocytes from mice treated with compounds *in vivo*; and Up in Hep + PCN, genes
523 selectively induced by the PXR agonist, PCN, compared with either vehicle (corn oil) or the CAR
524 agonist, TC, in hepatocytes from mice treated with compounds *in vivo*. Differential gene expression of
525 *in vitro*-differentiated Tr1 (GSE92940)[22] and Th17 cells (GSE21670)[36] were determined using the
526 Limma package in R (for microarray data)[37] to generate the gene sets: Tr1-signature, genes selectively
527 expressed in *in vitro*-differentiated Tr1 cells, compared with non-polarizing conditions; and Th17-
528 signature, genes selectively expressed in *in vitro*-differentiated Th17 cells, compared with non-
529 polarizing conditions. Th1-signature, Th2-signature, induced (i)Treg-signature (GSE14308)[38], or T
530 follicular helper (Tfh)-signature (GSE21379)[39], genes selectively induced in these *vs*. other T cell
531 subsets, as curated on MSigDB (https://www.gsea-msigdb.org/gsea/msigdb/index.jsp).
532

533 **TR-FRET co-regulator recruitment assay**

534 The DNA sequences encoding mouse (m)CAR ligand-binding domain (LBD; residues 109 – 358) were
535 amplified by PCR reaction and inserted into modified pET24b vectors to produce pET24b-mCAR-LBD.
536 pACYC-Duet1-RXR-LBD, an expression plasmid for untagged human (h)RXRα LBD was provided by
537 Dr. Eric Xu[40]. Purification of the mCAR-hRXRα LBD heterodimer, as well as hRXRα homodimer, was
538 achieved by nickel-affinity chromatography, followed by size-exclusion chromatography in an Akta
539 explorer FPLC (GE Healthcare). Briefly, pET24b-mCAR-LBD and pACYC-Duet1-RXR-LBD were co-
540 transformed into BL21 (DE3) for mCAR-hRXRα heterodimer and pET46-RXRα-LBD was transformed
541 into BL21 (DE3) for RXRα homodimer. The cells were grown in 4 x 900 mL of LB media at 37 °C until
542 the OD600 reached a value of 0.6–0.7. Overexpression was induced by 0.3 mM of IPTG and the cells
543 were grown further for 22 hr at 18 °C. The harvested cells were resuspended in sonication buffer (500
544 mM NaCl, 10 mM HEPES, 10 mM imidazole, pH 8.0, and 10% glycerol), sonicated on an ice-water
545 bath for 20 min at 18 W output, and centrifuged for 25 min at 50,000 x g. The proteins were isolated
546 from the sonicated supernatant by applying to a 2 mL His Select column and eluted with linear gradient

547 from 10 mM to 300 mM imidazole in sonication buffer. The elution fractions containing the proteins
548 concentrated while exchanging buffer to gel filtration buffer (300 mM NaCl, 20 mM HEPES, 1 mM
549 DTT, 5 % glycerol). The proteins were purified further by gel filtrations through a Superdex 200 26/60
550 column (GE Healthcare) equilibrated with gel filtration buffer. Fractions containing the proteins were
551 pooled and concentrated to ~ 8 mg/mL each with 30 kDa cutoff ultrafiltration units (Millipore). Time-
552 resolved fluorescence resonance energy transfer (TR-FRET) assays were performed in low-volume
553 black 384-well plates (Greiner) using 23 μL final well volume. Each well contained the following
554 components in TR-FRET buffer (20 mM KH_2PO_4/K_2HPO_4, pH 8, 50 mM KCl, 5 mM TCEP, 0.005%
555 Tween 20): 4 nM 6xHis-CAR/RXRα LBD heterodimer or 6xHis-RXRα/RXRα homodimer LBD, 1 nM
556 LanthaScreen Elite Tb-anti-His Antibody (ThermoFisher #PV5895), and 400 nM FITC-labeled PGC1α
557 peptide (residues 137–155, EAEEPSLLKKLLLAPANTQ, containing an N-terminal FITC label with a
558 six-carbon linker, synthesized by Lifetein). Pure ligand (TC, 9-*cis* RA) or tissue extracts (see above)
559 were prepared via serial dilution in vehicle (DMSO or PBS, respectively), and added to the wells along
560 with vehicle control. Plates were incubated at 25 °C for 1 hr and fluorescence was measured using a
561 BioTek Synergy Neo plate reader (Promega). The terbium (Tb) donor was excited at 340 nm, its emission
562 was monitored at 495 nm, and emission of the FITC acceptor was monitored at 520 nm. Data were
563 plotted as 520/340 nM rations using Prism software (GraphPad); TC data were fit to a sigmoidal dose
564 response curve equation.
565
566 **Quantification and Statistical Analyses**
567 Statistical analyses were performed using Prism (GraphPad). *P* values were determined by paired or
568 unpaired student's *t* tests, Log-rank test, one-way ANOVA, and two-way ANOVA analyses as
569 appropriate and as listed throughout the Figure legends. Statistical significance of differences (* $P <$
570 0.05, ** $P < 0.01$, *** $P < 0.001$, **** $P < 0.0001$) are specified throughout the Figure legends. Unless
571 otherwise noted in legends, data are shown as mean values ± S.E.M.
572

573 ## Data availability

574 RNA-seq data for wild type and CAR-deficient effector $CD4^+$ T cells from spleen, small intestine lamina
575 propria or colon lamina propria of congenically co-transferred *Rag1*$^{-/-}$ mice, as well as from human
576 peripheral blood $\alpha4^+\beta7^+CCR9^+$ memory $CD4^+$ T cells stimulated *ex vivo* in the presence or absence of
577 the human CAR agonist, CITCO, are available on the NCBI Gene Expression Omnibus (GEO)
578 repository (accession ID: GSE149220).

579 **Figure legends**

580

581 **Fig. 1. A pooled *in vivo* RNAi screen identifies CAR as a transcriptional regulator of MDR1**
582 **expression in mucosal T cells. (a)** Naïve $CD4^+$ T cells from spleens of wild type FVB/N mice (FVB
583 Tnaive), were activated and transduced in 96-well plates with a library of 258 retroviruses expressing
584 unique shRNAmirs against 70 genes together with the retroviral reporter, Ametrine (one shRNAmir
585 clone per well; see supplementary online information for details of the screening library). Transduced
586 cells were expanded until day 5, after which cells were pooled, FACS-sorted (as $Ametrine^+$ cells), and
587 transferred as a pool into FVB.*Rag1*$^{-/-}$ recipients; an aliquot of the pooled and sorted "input" cells (*i.e.*,
588 prior to *in vivo* transfer) was frozen for subsequent analysis. Viable transduced ($Ametrine^+$)
589 effector/memory (Teff; $CD4^+CD25^-CD62L^{lo}CD44^{hi}$) cells were re-isolated by FACS-sorting 6-weeks
590 post-T cell transfer from spleen or small intestine lamina propria (siLP). Total transduced spleen Teff
591 cells were collected, and both spleen and siLP Teff cells were further sub-divided into $Mdr1^{hi}$ and $Mdr1^{lo}$
592 subsets, based on efflux of the Mdr1 fluorescent substrate, Rh123. gDNA from all 6 Teff cell pools were
593 subjected to DNA-seq to quantify shRNAmir abundance. **(b)** Median $\log_2$ fold-change in abundance of
594 shRNAmirs in $Mdr1^{hi}$ *vs*. $Mdr1^{lo}$ siLP Teff cells. Dashed horizontal lines indicate 2-fold changes. Data
595 incorporates shRNAmir abundance, determined by DNA-seq, in 2-indpeendent screens using pooled
596 spleens and siLP from 10 transferred FVB.*Rag1*$^{-/-}$ mice per screen. **(c)** Diagram of the *Nr1i3*/CAR locus.
597 Seed sequence positions for each of the 5 shRNAmirs targeting CAR (*shNr1i3s*) are shown; 5' and 3'
598 untranslated regions (UTR) are indicated; filled boxes depict exons. **(d)** Mean weight loss ($\pm$ SEM) in
599 co-housed FVB.*Rag1*$^{-/-}$ mice injected with FVB wild type $CD4^+$ T cells transduced *in vitro* with a
600 negative control shRNAmir against CD8 (*shCd8a*; n = 11), or the indicated shRNAmirs against CAR
601 (*shNr1i3*s); *shNr1i3.1* (n = 7), *shNr1i3.2* (n = 7), *shNr1i3.3* (n = 7), *shNr1i3.4* (n = 7), *shNr1i3.5* (n = 7).
602 *** $P < .001$, **** $P < .0001$, Two-way ANOVA. **(e)** Correlation between mean weight loss induced
603 by Teff cells in FVB.*Rag1*$^{-/-}$ recipients (at 6-weeks post-T cell transfer; as in [d]) and mean percent of
604 Mdr1-dependent Rh123 efflux in *ex vivo*-isolated spleen Teff cells (determined by flow cytometry as in
605 Extended Data Fig. 1c-d). ** $P < .01$, Pearson (r) correlation test. **(f)** Mean weight loss ($\pm$ SEM) in
606 B6.*Rag2*$^{-/-}$ mice transplanted with naïve $CD4^+$ T cells from spleens of C57BL/6 wild type (B6; blue; n =
607 7) or CAR-deficient (B6.*Nr1i3*$^{-/-}$; red; n = 9) mice. ** $P < .01$, Two-way ANOVA. **(g)** H&E-stained
608 sections of colons or terminal ilea from co-housed B6.*Rag2*$^{-/-}$ mice 6-weeks after transfer of wild-type
609 (B6) or CAR-deficient (B6.*Nr1i3*$^{-/-}$) naïve $CD4^+$ T cells as in (f). Representative of 7-9 mice per group
610 from 2-independent experiments. **(h)** Mean histology scores ($\pm$ SEM) for colons or terminal ilea from

611 co-housed B6.*Rag2*$^{-/-}$ mice injected with wild-type (B6; n =7) or CAR-deficient (B6.*Nr1i3*$^{-/-}$; n = 9)
612 naïve CD4^{+} T cells as in (f-g). ** $P < .01$, two-tailed Mann-Whitney test.
613
614 **Fig. 2. CAR reprograms T cell gene expression in the small intestine. (a)** Equal numbers of CD45.1
615 wild type (B6; blue) and CD45.2 CAR-deficient (B6.*Nr1i3*$^{-/-}$; red) naïve CD4^{+} T cells were transferred
616 together into B6.*Rag1*$^{-/-}$ mice. Resulting T effector (Teff) cells were FACS-purified 3-weeks later from
617 spleen, small intestine lamina propria (siLP), or colon lamina propria (cLP) and transcriptional profiles
618 were assessed by RNA-seq. **(b)** Principle component analysis (PCA) of gene expression in *ex vivo*-
619 isolated wild type (B6) or CAR-deficient (B6.*Nr1i3*$^{-/-}$) Teff cells from spleen, siLP, or cLP of
620 congenically co-transferred B6.*Rag1*$^{-/-}$ mice as in (a). **(c)** *Top*, overlap, presented as Venn diagrams,
621 between genes expressed significantly higher in B6 wild type effector/memory (Teff) cells re-isolated
622 from spleen, small intestine lamina propria (siLP) or colon lamina propria (cLP) of week 3 T cell-
623 reconstituted B6.*Rag1*$^{-/-}$ mice (as in [a]), compared with each other. Genes expressed significantly higher
624 in spleen-, siLP- or cLP-derived wild type Teff cells, compared with wild type counterparts from the
625 other two tissues—referred to here as spleen, siLP or cLP Teff signature (sig) genes—were used for
626 downstream analyses. *Bottom*, differential genes expression, determined by DEseq2 and presented as
627 volcano plots, between wild type (B6) and CAR-deficient (B6.*Nr1i3*$^{-/-}$) Teff cells from the spleen, siLP
628 or cLP of week 3 T cell-reconstituted B6.*Rag1*$^{-/-}$ mice (as in [a]). Numbers of differentially-expressed
629 genes (Up; Down) are indicated in grey text for each comparison; examples of wild type siLP-signature
630 genes showing reduced expression in CAR-deficient *vs*. wild type Teff cells are annotated in green text.
631 **(d)** *Left*, gene set enrichment analysis (GSEA) showing that siLP B6 wild type Teff cell signature genes
632 (siLP B6 Teff sig; determined as in [c]) are significantly enriched within those expressed lower in
633 B6.*Nr1i3*$^{-/-}$ *vs*. wild type siLP Teff cells. Normalized enrichment score (NES) and P value is indicated.
634 *Right*, GSEA summary plot showing enrichment of tissue-specific (spleen, siLP, cLP) wild type Teff
635 cell signature genes (determined as in [c]; x-axis) within genes differentially expressed between CAR-
636 deficient (B6.*Nr1i3*$^{-/-}$) and wild type (B6) Teff cells from spleen, siLP or cLP (y-axis). Circle sizes are
637 proportional to -$\log_{10}$ adjusted P (Padj) values; color represents directionality of enrichment, based on
638 NES. (b-d) Mean normalized gene expression values, expressed as TPM, are shown from 3-independent
639 experiments using Teff cells purified from pooled tissues of 5 congenically co-transferred B6.*Rag1*$^{-/-}$
640 mice per experiment. **(e)** Mean relative expression ($\pm$ SEM; n = 3) of *Abcb1a* or *Cyp2b10*, determined
641 by qPCR, in wild type (B6) or CAR-deficient (B6.*Nr1i3*$^{-/-}$) Teff cells re-isolated from spleens of
642 congenically co-transferred B6.*Rag1*$^{-/-}$ mice (as in [a]) and stimulated *ex vivo* with anti-CD3/anti-CD28
643 antibodies in the presence or absence of tissue extracts isolated from wild type (B6) mice. Veh, vehicle;

644 TC, CAR agonist TCPOBOP; siLC, small intestine lumen content; bile, from gallbladder; cLC, colon
645 lumen content. * $P < .05$, ** $P < .01$, *** $P < .001$, One-way ANOVA with Dunett's correction for
646 multiple comparisons. NS, not significant. **(f)** Mean activation (± SEM; triplicate samples) of
647 recombinant mouse (m)CAR-human (h)RXRα ligand-binding domain (LBD) heterodimers, determined
648 by time-resolved fluorescence resonance energy transfer (TR-FRET), in the presence of the mCAR
649 agonist, TCPOBOP (TC; blue) or the hRXRα agonist, 9-*cis* retinoic acid (RA; red). Median effective
650 concentrations (EC_{50}'s) of TC-dependent bi-phasic mCAR:hRXRα LBD heterodimer activation are
651 indicated. Representative of more than 5-independent experiments. **(g)** Mean activation (± SEM; $n = 3$)
652 of mCAR:hRXRα LBD heterodimers, determined by TR-FRET as in (f), in the presence of titrating
653 concentrations of siLC, bile, cLC or serum from wild type B6 mice. The 4 bars for each tissue extract
654 are *(left to right)*: (1) diluent (PBS) alone; (2) 0.01%, (3) 0.1%, and (4) 1%. Data are shown from 3-
655 independent experiments using extracts from different wild type mice; each concentration from each
656 individual mouse was run in triplicate. * $P < .05$, **** $P < .0001$, one-way ANOVA with Tukey's
657 correction for multiple comparisons. NS, not significant.
658
659 **Fig. 3. CAR promotes *Il10* gene expression in T cells. (a)** Gene set enrichment analysis (GSEA)
660 showing enrichment of genes previously associated with type 1 regulatory (Tr1) cells[21] amongst those
661 expressed at lower levels in CAR-deficient (B6.*Nr1i3*$^{-/-}$) *vs*. wild type (B6) small intestine lamina propria
662 (siLP) Teff cells (as in Fig. 2a-d). Normalized enrichment score (NES) and *P* value are listed. **(b)** GSEA
663 summary plot showing enrichment of gene sets previously assigned to major effector and regulatory T
664 cell lineages (see methods for details) within genes differentially expressed between CAR-deficient
665 (B6.*Nr1i3*$^{-/-}$) and wild type (B6) Teff cells from spleen, siLP or cLP (y-axis). Circle sizes reflect -$\log_{10}$
666 adjusted *P* (Padj) values; color represents directionality of enrichment, based on NES. **(c)** *Ex vivo Il10*
667 gene expression, displayed as transcripts per million (TPM) and determined by RNA-seq ($n = 3$), in *ex*
668 *vivo*-isolated wild type (B6; blue) or CAR-deficient (B6.*Nr1i3*$^{-/-}$; red) Teff cells from spleen, siLP, or
669 cLP of congenically transferred B6.*Rag1*$^{-/-}$ mice (as in Fig. 2a). *P* values (paired two-tailed student's *t*
670 test) are indicated. **(d)** *Left*, equal numbers of CD45.1 CAR-sufficient (10BiT; blue) and CD45.2 CAR-
671 deficient (*Nr1i3*$^{-/-}$ 10BiT; red) *Il10*-Thy1.1 reporter naïve CD4^{+} T cells were transferred together into
672 B6.*Rag1*$^{-/-}$ mice. Expression of the *Il10* reporter (10BiT) allele in Teff cells from spleen, siLP, or cLP
673 was analyzed after 2 weeks by *ex vivo* flow cytometry analysis of Thy1.1 expression. *Right*, *Il10*
674 expression, identified by Thy1.1 staining, in CD45.1^{+} CAR-sufficient or CD45.1^{-} (CD45.2) CAR-
675 deficient Teff cells from spleen, siLP, or cLP of week 2 reconstituted *Rag1*$^{-/-}$ mice. Representative of 4

676 mice analyzed over 2-independent experiments. **(e)** Mean percentages (n = 4; ± SEM) of Thy1.1 (*Il10*)-
677 expressing wild type (B6, blue) or CAR-deficient (B6.*Nr1i3*$^{-/-}$) spleen, siLP, or cLP Teff cells,
678 determined by *ex vivo* flow cytometry as in (d). * $P < .05$, ** $P < .01$, One-way ANOVA with Tukey's
679 correction for multiple comparisons. **(f)** Mean relative *Il10* expression (± SEM; n = 3), determined by
680 qPCR, in wild type (B6) or CAR-deficient (B6.*Nr1i3*$^{-/-}$) Teff cells re-isolated from spleens of
681 congenically co-transferred B6.*Rag1*$^{-/-}$ mice (as in Fig. 2a, 2e) and stimulated *ex vivo* with anti-CD3/anti-
682 CD28 antibodies in the presence or absence of tissue extracts isolated from wild type (B6) mice. Veh,
683 vehicle; TC, CAR agonist TCPOBOP; siLC, small intestine lumen content; bile, from gallbladder; cLC,
684 colon lumen content. * $P < .05$, ** $P < .01$, *** $P < .001$, One-way ANOVA with Tukey's correction
685 for multiple comparisons. NS, not significant. **(g)** Mean relative CAR/*Nr1i3* gene expression (± SEM; n
686 = 2), determined by qPCR, in B6 wild type naïve CD4^{+} T cells cultured for 4 days in polarizing
687 conditions to generate effector or regulatory T cell subsets. Tr1 conditions included cells activated and
688 expanded in the presence of IL-27 alone, dexamethasone (Dex) alone, or both together. npTh17, non-
689 pathogenic Th17 cells; pTh17, pathogenic Th17 cells. **(h)** IL-10 and IFNγ expression in CD45.1 wild
690 type (B6) or CD45.2 CAR-deficient (B6.*Nr1i3*$^{-/-}$) T cells activated and expanded together for 4 days in
691 media alone, IL-27 alone, dexamethasone (Dex) alone, or IL-27 plus Dex. Cytokine expression was
692 analyzed by intracellular cytokine staining after restimulation with PMA and ionomycin (see methods);
693 representative of 5 experiments. Numbers indicate percentages. **(i)** Mean percentages (n = 5; ± SEM) of
694 IL-10-expressing wild type (B6) or CD45.2 CAR-deficient (B6.*Nr1i3*$^{-/-}$) T cells after 4-day co-culture
695 as in (h). * $P < .05$, paired two-tailed student's t test.
696
697 **Fig. 4. Pharmacologic CAR activation suppresses bile acid-induced experimental ileitis. (a)** Mean
698 relative expression (± SEM; n = 3) of *Abcb1a*, *Cyp2b10*, or *Il10*, determined by qPCR, in wild type (B6;
699 blue) or CAR-deficient (B6.*Nr1i3*$^{-/-}$; red) Teff cells isolated from spleens of congenically co-transferred
700 B6.*Rag1*$^{-/-}$ mice 72 hr after a single dose of either the CAR agonist, TCPOBOP (TC), or vehicle. Data
701 are shown as relative expression in Teff cells from TC- *vs*. vehicle-treated mice; individual data points
702 reflect 3-independent TC treatment experiments in which wild type or CAR-deficient Teff cells were
703 isolated from a pool of 5 spleens isolated from identically treated animals. * $P < .05$, paired two-tail
704 student's t test. **(b)** Mean weight loss (± SEM) of co-housed *Rag2*$^{-/-}$ mice transplanted with wild-type
705 naïve T cells and maintained on a CA-supplemented diet with (red; n = 18) or without (blue; n = 16) TC
706 treatment. CA-fed *Rag2*$^{-/-}$ mice not reconstituted with T cells (no T cells; grey; n =10), or *Rag2*$^{-/-}$ mice
707 transplanted with wild type T cells and left on control chow diet treated with vehicle (black, n = 17) are

708 also shown. Weights are presented relative to the start of TC treatment (3-weeks post-T cell transfer). *
709 $P < .05$, ** $P < .01$, Two-way ANOVA. **(c)** *Top,* H&E-stained sections of terminal ilea or colons from
710 control or CA-fed *Rag2*$^{-/-}$ mice reconstituted with wild type T cells and treated +/- TC as in (b).
711 Representative of 3-4 mice/group. *Bottom,* mean histology scores (± SEM) for colons (n = 3-4) or
712 terminal ilea (n = 3) as in (c). * $P < .05$, one-way ANOVA with Tukey's correction for multiple
713 comparisons. NS, not significant. **(d)** Model of CAR-dependent mucosal T cell regulation in the small
714 intestine. Bile acids reabsorbed by enterocytes in the ileum expressing the Apical sodium-dependent bile
715 acid transporter (Asbt) accumulate in the lamina propria, inducing stress and inflammation, which may
716 increase CAR expression in mucosal Teff cells. Other (non-BA) metabolites in bile directly activate the
717 CAR ligand-binding domain (LBD), leading to increased expression of at least two discrete, yet
718 functionally synergistic gene sets, which serve to detoxify BAs (e.g., MDR1Abcb1a, cytochrome P450
719 enzymes [CYPs]), suppress inflammation via IL-10 and support small bowel immune homeostasis.
720

721 **Extended Data Figure Legends**

722

723 **Extended Data Figure 1. Nuclear receptor-dependent regulation of effector T cell persistence and**
724 **MDR1 expression *in vivo*. (a)** *Top*, abundance of shRNAmirs in *ex vivo*-isolated spleen and *in vitro*-
725 transduced (input) Teff cells. shRNAmirs with ≤ 1 normalized read in both *ex vivo* spleen and input Teff
726 cell pools were considered 'poorly represented' (highlighted green). Well-represented shRNAmirs
727 displaying ≤ 10-fold change between *ex vivo* spleen and input Teff cell pools (between blue lines) were
728 considered for downstream analysis. *Bottom*, abundance of shRNAmirs, filtered for minimal effects on
729 *in vivo* Teff cell persistence, in *ex vivo*-isolated Mdr1^{hi} (Rh123^{lo}) and Mdr1^{lo} (Rh123^{hi}) siLP Teff cells.
730 **(b)** Log_2 fold-change in abundance (± SEM) of shRNAmirs against *Cd19* (n = 3), *Abcb1a* (n = 2), *Nr1i3*
731 (n = 5), *Thra* (n = 6), and *Esrra* (n = 3) in FVB wild type Rh123^{lo} (MDR1^{hi}) *vs*. Rh123^{hi} (MDR1^{lo})
732 effector/memory T cells (Teff; sorted as in Fig. 1a) recovered from spleens or small intestine lamina
733 propria (siLP) of transferred FVB.*Rag1*$^{-/-}$ mice. (a-b) Data incorporates shRNAmir abundance,
734 determined by DNA-seq, in 2-indpeendent screens using pooled spleens and siLP from 10 transferred
735 FVB.*Rag1*$^{-/-}$ mice per screen. **(c)** *Ex vivo* Rh123 efflux, determined by flow cytometry, in FVB wild type
736 Teff cells expressing a control shRNAmir against CD8 (*shCD8a*) or 1 of 5-independent shRNAmirs
737 against CAR (*shNr1i3*) isolated from spleens of transferred FVB.*Rag1*$^{-/-}$ mice 6-weeks post-transfer.
738 Rh123 efflux in transduced (Ametrine pos.; blue) cells is overlaid with that in congenically-transferred
739 untransduced (Ametrine neg.; red) Teff cells from the same mouse. Background Rh123 efflux in

740 untransduced Teff cells treated with the MDR1 inhibitor, elacridar, is shown in gray. Representative of
741 63 mice analyzed over 3-independent experiments. **(d)** Mean normalized *ex vivo* Rh123 efflux (± SEM)
742 in FVB wild type spleen Teff cells expressing control (*shCd8a*; *n* = 11) or CAR-targeting (shNr1i3)
743 shRNAmirs; *shNr1i3.1* (*n* = 10), *shNr1i3.2* (*n* = 10), *shNr1i3.3* (*n* = 12), *shNr1i3.4* (*n* = 10), *shNr1i3.5*
744 (*n* = 10), determined by flow cytometry as in (c). Rh123 efflux was normalized to control *shCd8a*-
745 expressing Teff cells after calculating the change (Δ) in Rh123 mean fluorescence intensity (MFI)
746 between congenically-transferred transduced (ametrine pos.) *vs*. untransduced (ametrine neg.) Teff cells.
747 * $P < .05$, **** $P < .0001$, One-way ANOVA with Dunnett's correction for multiple comparisons. **(e)**
748 Mean relative *Abcb1a*, *Nr1i3*, and *Cyp2b10* expression (± SEM), determined by qPCR, in FVB spleen
749 Teff cells FACS-sorted from FVB.*Rag1*$^{-/-}$ recipient mice expressing either a negative control shRNAmir
750 against CD8 (*shCd8a*; *n* = 8), or the indicated shRNAmirs against CAR (*shNr1i3*s); *shNr1i3.1* (*n* = 8),
751 *shNr1i3.2* (*n* = 8), *shNr1i3.3* (*n* = 8), *shNr1i3.4* (*n* = 8), *shNr1i3.5* (*n* = 8).* $P < .05$, ** $P < .01$, *** $P <$
752 $.001$, **** $P < .0001$, One-way ANOVA with Tukey's correction for multiple comparisons. **(f)** Median
753 $\log_2$ fold change in shRNAmir abundance between FVB wild type *ex vivo*-isolated spleen *vs*. *in vitro*-
754 transduced (input) Teff cells. (a, d) shRNAmir abundance reflects the mean number of normalized reads,
755 by DNA-seq, in the indicated Teff subsets obtained in 2-independent screens, each using cells transferred
756 into 10 FVB.*Rag1*$^{-/-}$ mice. **(g)** *Ex vivo* Rh123 efflux, determined by flow cytometry, in CD45.1 wild type
757 (B6; red) or CD45.2 CAR-deficient (B6.*Nr1i3*$^{-/-}$), PXR-deficient (B6.*Nr1i2*$^{-/-}$) or CAR/PXR double-
758 deficient (B6.*Nr1i3*$^{-/-}$*Nr1i2*$^{-/-}$) effector/memory T cells (Teff; gated as in Extended Data Fig. 8a; blue)
759 isolated from spleens of B6.*Rag1*$^{-/-}$ mice 6-weeks post-naïve T cell congenic co-transfer. Background
760 Rh123 efflux in CD45.1 B6 Teff cells treated with the MDR1 inhibitor, elacridar, is shown in gray.
761 Representative of a total of 22 mice analyzed over two-independent T cell transfer experiments. **(h)**
762 Mean normalized Rh123 efflux (± SEM) in congenically-transferred CD45.1 wild type (B6; *n* = 7) or
763 CD45.2 CAR-deficient (B6.*Nr1i3*$^{-/-}$; *n* = 7), PXR-deficient (B6.*Nr1i2*$^{-/-}$; *n* = 7) or CAR/PXR double-
764 deficient (B6.*Nr1i3*$^{-/-}$*Nr1i2*$^{-/-}$; *n* = 7) spleen Teff cells, determined by flow cytometry as in (g). * $P < .05$,
765 One-way ANOVA with Tukey's correction for multiple comparisons. **(i)** Mean relative *Abcb1a*
766 expression (± SEM), determined by *ex vivo* qPCR, in CD45.1 wild type (B6; *n* = 5) or CD45.2 CAR-
767 deficient (B6.*Nr1i3*$^{-/-}$; *n* = 5), PXR-deficient (B6.*Nr1i2*$^{-/-}$; *n* = 4) or CAR/PXR double-deficient
768 (B6.*Nr1i3*$^{-/-}$*Nr1i2*$^{-/-}$; *n* = 5) spleen Teff cells (sorted as in Extended Data Fig. 8a) from spleens of
769 congenically-transferred B6.*Rag1*$^{-/-}$ as in (a). * $P < .05$, One-way ANOVA with Tukey's correction for
770 multiple comparisons.
771

772 **Extended Data Figure 2. Inhibition of bile acid reabsorption rescues ileitis induced by CAR-**
773 **deficient T cells in reconstituted *Rag*$^{-/-}$ mice. (a)** Mean weight loss (±SEM) of co-housed B6.*Rag2*$^{-/-}$
774 mice transplanted with wild type (B6; blue; n = 15) or CAR-deficient (B6.*Nr1i3*$^{-/-}$; red; n = 13) naïve
775 CD4^{+} T cells and treated with 2% (w:w) cholestyramine (CME) beginning at 3-weeks post-T cell
776 transfer. NS, not significant. **(b)** *Top*, H&E-stained sections of colons or terminal ilea from B6.*Rag2*$^{-/-}$
777 mice reconstituted with wild type or CAR-deficient T cells and treated +/- CME as in (a). Representative
778 of 12 mice/group. *Bottom*, mean histology scores (± SEM; n = 12) for colons or terminal ilea as in (a).
779 NS, not significant. **(c)** Mean weight loss (±SEM) of co-housed B6.*Rag1*$^{-/-}$ mice with or without the
780 Apical sodium-dependent bile acid transporter (Asbt; gene symbol *Slc10a2*) after transplantation with
781 wild type (B6; blue) or CAR-deficient (B6.*Nr1i3*$^{-/-}$; red) naïve CD4^{+} T cells. **(d)** *Top*, H&E-stained
782 sections of terminal ilea or colons from control or Asbt-deficient B6.*Rag1*$^{-/-}$ mice reconstituted with wild
783 type or CAR-deficient T cells as in (c). Representative of 5 mice/group. *Bottom*, mean histology scores
784 (± SEM; n = 5) for colons or terminal ilea as above. * $P < .05$, ** $P < .01$, *** $P < .001$, One-way
785 ANOVA with Tukey's correction for multiple comparisons. NS, not significant.
786
787 **Extended Data Figure 3. Shared features of CAR-dependent gene expression in mucosal T cells**
788 **and hepatocytes. (a)** Overlap, presented as Venn diagrams, between genes induced in B6 wild type
789 mouse hepatocytes by *in vivo* treatment with either the mouse CAR agonist, TCPOBOP (TC) or the
790 mouse PXR agonist, PCN, relative to vehicle (CO, corn oil). **(b)** Summary gene set enrichment analysis
791 (GSEA) plot showing that genes induced by TC, but not PCN, treatment in mouse hepatocytes (as in
792 [a]), are enriched within those expressed at lower levels in CAR-deficient (B6.*Nr1i3*$^{-/-}$) *vs*. wild type
793 (B6) siLP Teff cells from week-3 congenically co-transferred *Rag1*$^{-/-}$ mice (as in Fig. 2a-c). Normalized
794 enrichment scores (NES) and P values are indicated by circle color and size, respectively. **(c)** Differential
795 gene expression, determined by DEseq2 and shown as a volcano plot, between CAR-deficient (B6.*Nr1i3*$^{-}$
796 $^{/-}$) and wild type (B6) siLP Teff cells re-isolated from transferred B6.*Rag1*$^{-/-}$ mice, as in Fig. 2a. Genes
797 induced by TC, but not PCN, treatment in mouse hepatocytes (as in [a]; purple), bound by CAR in ChIP-
798 seq analysis of hepatocytes from TC-treated mice (blue), or both (red) are highlighted. Chi-square P
799 values are indicated. **(d)** CAR-occupancy, determined by ChIP-seq, at representative loci whose
800 expression is regulated by CAR in both mucosal T cells and hepatocytes within mouse hepatocytes
801 ectopically expressing epitope-tagged mouse (m) or human (h) CAR proteins and re-isolated from mice
802 after treatment with the mCAR agonist, TCPOBOP (TC), or the hCAR agonist, CITCO. * $P < 0.00001$;
803 significant binding peaks were called in MACS using base settings.
804

805 **Extended Data Figure 4. CAR promotes effector T cell persistence in the presence of small**
806 **intestinal bile acids**. **(a)** Percentages of live CD44^{hi} wild type (B6; CD45.1^{+}; blue) or CAR-deficient
807 (B6.*Nr1i3*$^{-/-}$; CD45.1^{-}; red) effector/memory (Teff) cells, determined by flow cytometry and gated as in
808 Extended Data Fig. 8a, in tissues of reconstituted B6.*Rag1*$^{-/-}$ mice over time. Numbers indicate
809 percentages; representative of 5 mice per tissue and timepoint. **(b)** Fitness, defined as mean $\log_2$ fold-
810 change (F.C.) of CAR-deficient (B6.*Nr1i3*$^{-/-}$) *vs*. wild type (B6) Teff cell percentages ($\pm$ SEM; $n = 5$) in
811 tissues of congenically co-transferred *Rag1*$^{-/-}$ mice over time, determined by flow cytometry as in (a).
812 **(c)** Percentage of wild type (B6, CD45.1^{+}; blue) and CAR-deficient (B6.*Nr1i3*$^{-/-}$, CD45.1^{-}; red) naïve
813 (CD62L^{hi}) CD4^{+} T cells after sorting and mixing, and prior to *in vivo* transfer into *Rag1*$^{-/-}$ mice (input
814 Tnaive); representative of 3 mixtures used for analyzing resulting Teff cells at 2- 4- or 6-weeks post-
815 transfer. **(d)** Equal numbers of CD45.1 wild type (B6; blue) and CD45.2 CAR-deficient (B6.*Nr1i3*$^{-/-}$;
816 red) naïve CD4^{+} T cells were transferred together into co-housed *Rag1*$^{-/-}$ mice with or without the ileal
817 bile acid reuptake transporter, Asbt (gene symbol *Slc10a2*). Resulting effector (Teff) cells from small
818 intestine lamina propria (siLP) were analyzed 2-weeks post- T cell transfer via flow cytometry. **(e)**
819 Percentages of live CD44^{hi} wild type (B6; CD45.1^{+}; blue) or CAR-deficient (B6.*Nr1i3*$^{-/-}$; CD45.1^{-}; red)
820 effector/memory (Teff) cells, determined by flow cytometry and gated as in Extended Data Fig. 8a, in
821 siLP of week-2 reconstituted B6.*Rag1*$^{-/-}$ mice. Numbers indicate percentages; representative of 8-10
822 mice analyzed over two-independent experiments. **(f)** Mean absolute numbers ($\pm$ SEM) of live CD45.1
823 wild type (B6; *left*) or CD45.2 CAR-deficient (B6.*Nr1i3*$^{-/-}$; *right*) Teff cells, determined by *ex vivo* flow
824 cytometry as in (e), from siLP 2-weeks after mixed T cell transfer into control (Asbt$^{+/+}$; blue; $n = 8$) or
825 Asbt-deficient (Asbt$^{-/-}$; red; $n = 10$) *Rag1*$^{-/-}$ recipients. Fold-changes in cell numbers recovered from
826 Asbt-deficient *vs*. control recipients, as well as *P* values (two-tailed unpaired student's t test) are
827 indicated.
828
829 **Extended Data Figure 5. Preferential CAR expression and function in human effector/memory T**
830 **cells expressing small bowel homing receptors. (a)** FACS-based identification of human CD4^{+} T cell
831 subsets in PBMC from healthy adult human donors. Expression of integrin α4 (α4 int.) in gated naïve
832 (gray), T regulatory (Treg; blue), or effector/memory (Teff; red) T cells is shown at right. **(b)** Expression
833 of integrin β7 (β7 int.) and CCR9 in total naïve CD4^{+} T cells, or in α4 int.+/- Treg or Teff subsets (gated
834 as in (a)). Representative of 13-independent experiments using PBMC from different donors. **(c)**
835 Percentages (%) of α4^{+}β7^{+}CCR9^{+} Tnaive, Treg, or Teff cells, determined by flow cytometry as in (a-b).
836 Individual data points for the 13 independent experiments are shown and connected by grey lines. ** *P*

837 < .01, One-way ANOVA with Holm-Sidak's correction for multiple comparisons. **(d)** *Ex vivo* Rh123
838 efflux in $CD4^+$ T cell subsets (gated as in a-b) in the presence (gray) or absence (red) of the selective
839 MDR1 inhibitor, elacridar. Representative of 8 experiments. **(e)** Mean percentages (± SEM; n = 7) of
840 $Rh123^{lo}$ ($MDR1^+$) Teff subsets, determined by flow cytometry as in (d). * $P < .05$, ** $P < .01$, *** $P <$
841 .001, One-way ANOVA with Tukey's correction for multiple comparisons. **(f)** Mean (± SEM) *ex vivo*
842 expression, determined by qPCR, of CAR/*NR1I3* (n = 12), MDR1/*ABCB1* (n = 12) or *CYP2B6* (n = 10)
843 in $\alpha4^-\beta7^-CCR9^-$ or $\alpha4^+\beta7^+CCR9^+$ Tnaive, Treg or Teff cells, FACS-sorted as in (a-b). (e-f) * $P < .05$,
844 ** $P < .01$, One-way ANOVA with Tukey's correction for multiple comparisons. **(g)** Mean relative
845 *CYP2B6* expression (± SEM; n = 5), determined by qPCR, in $CD4^+$ T cell subsets (as in (f)) activated *ex*
846 *vivo* with anti-CD3/anti-CD28 antibodies in the presence or absence of titrating concentrations of the
847 human CAR agonist, CITCO. Gene expression was analyzed 24 hr post-activation. *** $P < .001$, Two-
848 way ANOVA. **(h)** Mean normalized MDR1/*ABCB1* or *CYP2B6* expression (± SEM), determined by
849 RNA-seq and presented as transcripts per million (TPM), in FACS-sorted $\alpha4^+\beta7^+CCR9^+$ Teff cells
850 stimulated *in vitro* (anti-CD3/anti-CD28) for 24 hr in the presence or absence of CITCO. Data from 4
851 replicate RNA-seq experiments are shown; ** $P < .001$, paired two-tailed student's t test. **(i)**
852 Identification of $CD4^+$ naive (Tnaive; $CD25^-CD45RO^-$; grey) or effector/memory (Teff; $CD25^-$
853 $CD45RO^+$; red) cells, by flow cytometry, from healthy adult human PBMC. For improved purity of Th1,
854 Th2, Th17 and Th17.1 cells, CCR10-expressing Th22 cells were excluded. CCR6 expression in Tnaive
855 (grey) or non-Th22 Teff cells (red) is shown at right; $CCR6^+$ or $CCR6^-$ Teff cells were gated to enrich
856 for Th17 or non-Th17 lineages, respectively. **(j)** Expression of CCR4 and CXCR3 in $CCR6^-$ (non-Th17;
857 *left*) or $CCR6^+$ (Th17; *right*) Teff cells identifies enriched $CCR6^-CCR4^{lo}CXCR3^{hi}$ (Th1; orange), $CCR6^-$
858 $CCR4^{hi}CXCR3^{lo}$ (Th2; blue), $CCR6^+CCR4^{hi}CXCR3^{lo}$ (Th17; green), and $CCR6^+CCR4^{lo}CXCR3^{hi}$
859 (Th17.1; red) subsets. **(k)** Expression of integrin α4 (α4 int.; *top*) in Th2, Th1, Th17 and Th17.1 human
860 Teff cells gated as in (a-b). Expression of integrin β7 (β7 int.) and CCR9 within α4 int^- (*middle*) or α4
861 int^+ (*bottom*) Th2, Th1, Th17 or Th17.1 cells gated as above. (a-c) Representative of 9-independent
862 experiments using PBMC from different healthy adult donors. **(l)** Percentages (n = 9) of $\alpha4^+\beta7^+CCR9^+$
863 cells within *ex vivo* Th1, Th2, Th17, or Th17.1 Teff cells gated as in (a-c). Data from independent donors
864 are connected by red lines. **(m)** MDR1-dependent Rh123 efflux in the indicated Th1, Th2, Th17, or
865 Th17.1 Teff subsets gated based on expression of α4 int., β7 int., and/or CCR9 in the presence (grey) or
866 absence (red) of elacridar. Representative of 8 independent experiments using PBMC from different
867 donors. **(n)** Mean percentages (± SEM; n = 8) of $Rh123^{lo}$ ($MDR1^+$) cells within Th1, Th2, Th17, or
868 Th17.1 Teff subsets gated based on expression of α4 int., β7 int., and/or CCR9 as in (e). * $P < .05$, ** P

869 < .01, *** P < .001, One-way ANOVA with Tukey's correction for multiple comparisons. ND, not
870 detectable; NS, not significant.
871
872 **Extended Data Figure 6. TCPOBOP promotes CAR-dependent gene expression in *ex vivo*-isolated**
873 **effector T cells. (a)** *Top left,* equal numbers of CD45.1 wild type (B6; blue) and CD45.2 CAR-deficient
874 (B6.*Nr1i3*$^{-/-}$; red) naïve CD4^{+} T cells were transferred together into B6.*Rag1*$^{-/-}$ mice. Resulting effector
875 (Teff) cells were FACS-purified from spleen after 3 weeks. *Right*, sequential gating strategy for re-
876 isolating wild type and CD45.2 CAR-deficient spleen Teff cells is shown. *Bottom left*, mean relative
877 *Abcb1a*, *Cyp2b10*, or *Il10* expression (± SEM; n = 4), determined by qPCR, in *ex vivo*-isolated wild type
878 (B6) or CAR-deficient (B6.*Nr1i3*$^{-/-}$) spleen Teff cells. These cells were used for *ex vivo* cell culture
879 experiments in the presence or absence of small molecule ligands ([b-c] below). * P < .05, ** P < .01,
880 paired two-tailed student's t test. **(b)** Mean relative expression (± SEM) of *Abcb1a* (n = 4), *Cyp2b10* (n
881 = 4), or *Il10* (n = 3), determined by qPCR, in wild type (B6) or CAR-deficient (B6.*Nr1i3*$^{-/-}$) Teff cells
882 isolated from transferred *Rag1*$^{-/-}$ mice (as in [a]), and stimulated *ex vivo* with anti-CD3/anti-CD28
883 antibodies (for 24 hr) in the presence or absence of the mouse (m)CAR agonist, TCPOBOP (TC; 10
884 μM), the mCAR inverse agonist, 5α-Androstan-3β-ol (And; 10 μM), or both. ** P < .01, *** P < .001,
885 **** P < .0001, one-way ANOVA with Tukey's correction for multiple comparisons. **(c)** Mean relative
886 *Abcb1a*, *Cyp2b10*, or *Il10* expression (± SEM; n = 5), determined by qPCR, in wild type (B6) or CAR-
887 deficient (B6.*Nr1i3*$^{-/-}$) Teff cells isolated and stimulated as in (a-b) in the presence or absence of TC (10
888 μM) or the mouse PXR agonist, PCN (10 μM). Data are presented as fold-change in mRNA abundance
889 relative to vehicle-treated cells (DMSO for TC; ethanol for PCN). **** P < .0001, one-way ANOVA
890 with Dunnett's correction for multiple comparisons. NS, not significant.
891
892 **Extended Data Figure 7. Characteristics of endogenous intestinal metabolites that activate the**
893 **CAR ligand-binding domain. (a)** Mean activation (± SEM; triplicate samples) of recombinant human
894 (h)RXRα ligand-binding domain (LBD) homodimers, determined by time-resolved fluorescence
895 resonance energy transfer (TR-FRET), in the presence of the mCAR agonist, TCPOBOP (TC; blue) or
896 the hRXRα agonist, 9-*cis* retinoic acid (RA; red). Median effective concentration (EC_{50}) of 9-*cis* RA-
897 dependent hRXRα LBD homodimer activation is indicated. Representative of more than 5-independent
898 experiments. **(b)** Mean activation (± SEM; n = 3) of hRXRα LBD homodimers, determined by TR-
899 FRET as in (a), in the presence of titrating concentrations of siLC, bile, cLC or serum from wild type B6
900 mice. * P < .05, **** P < .0001, one-way ANOVA with Tukey's correction for multiple comparisons.

901 NS, not significant. **(c)** Mean activation (± SEM; n = 3) of CAR:RXR LBD heterodimers, determined
902 by TR-FRET, in the presence of titrating concentrations of siLC isolated from conventionally-housed
903 (Conv) or germ-free (GF) wild type B6 mice pre-treated with or without cholestyramine (CME) to
904 deplete free bile acids. *** $P < .001$, **** $P < .0001$, One-way ANOVA with Dunnett's correction for
905 multiple comparisons. (a-c) The bars for each tissue extract indicate dilution series *(left to right)*: (1)
906 diluent (PBS) alone; (2) 0.01%, (3) 0.1%, and (4) 1%. Data are shown from 3-independent experiments
907 using extracts from different wild type mice, with each concentration from each individual mouse run in
908 triplicate. **(d)** Mean TR-FRET signals (± SEM; n = 3) of CAR:RXR LBD heterodimers in the presence
909 of titrating concentrations of individual bile acid (BA) species. NS, not significant, one-way ANOVA
910 with Dunnett's correction for multiple comparisons. The bars for BAs indicate concentrations *(left to*
911 *right)*: (1) vehicle (DMSO); (2) 10 μM; (3) 100 μM; and (4) 1000 μM. Data are shown from 3-
912 independent experiments, where each BA concentration was run in triplicate.
913
914 **Extended Data Figure 8. CAR is required for a transient wave of IL-10 production by mucosal T**
915 **cells early after naïve T cell transfer into *Rag*$^{-/-}$ mice.** **(a)** Equal numbers of CD45.1 wild type (B6;
916 blue) and CD45.2 CAR-deficient (B6.*Nr1i3*$^{-/-}$; red) naïve CD4^{+} T cells were transferred together into
917 *Rag1*$^{-/-}$ mice. Resulting effector (Teff) cells were analyzed—using surface and intracellular flow
918 cytometry after *ex vivo*-stimulation with phorbol myristate acetate (PMA) and ionomycin—at 2- 4- and
919 6-weeks from spleen, mesenteric lymph node (MLN), small intestine lamina propria (siLP), or colon
920 lamina propria (cLP). Gating hierarchy is shown from a representative sample of MLN mononuclear
921 cells at 2-weeks post-T cell transfer. **(b)** Intracellular IL-10 and IFNγ expression, determined by flow
922 cytometry, in wild type (B6, blue; *left*) or CAR-deficient (B6.*Nr1i3*$^{-/-}$, red; *right*) non-Th17 Teff cells,
923 gated as in (a), from tissues of T cell-reconstituted B6.*Rag1*$^{-/-}$ mice over time. Numbers indicate
924 percentages; representative of 5 mice per tissue and time point. Mean percentages **(c)** or numbers **(d)** (±
925 SEM; n = 5) of IL-10-expressing wild type (B6, *left*) or CAR-deficient (B6.*Nr1i3*$^{-/-}$, *right*) Teff cells,
926 determined by *ex vivo* flow cytometry as in (a-b), from tissues of transferred B6.*Rag1*$^{-/-}$ mice over time.
927 **(e)** Specificity of IL-10 intracellular staining, as validated by analysis of IL-10 production by CD45.1
928 wild type (B6; blue) or CD45.2 *Il10*$^{-/-}$ (red) Teff cells isolated from spleen or siLP of congenically co-
929 transferred *Rag1*$^{-/-}$ mice. Representative of 6 mice analyzed over 2-independent experiments. **(f)**
930 Percentages of CD3^{+}CD4^{+} T cells in tissues of *Rag1*$^{-/-}$ mice transplanted with congenic mixtures of wild
931 type and CAR-deficient naïve CD4^{+} T cells over time, determined by flow cytometry as in Extended
932 Data Fig. 11a. Representative of 5 mice per tissue and time point. **(g)** Mean absolute numbers of

933 $CD3^+CD4^+$ T helper (T_H) cells (± SEM; n = 5) in tissues of transferred B6.*Rag1*$^{-/-}$ mice over time,
934 determined by flow cytometry as in (a). **(h)** Mean relative *ex vivo* CAR (*Nr1i3*), MDR1 (*Abcb1a*),
935 *Cyp2b10*, or *Il10* gene expression (± SEM; n = 3), determined by qPCR, in wild type (B6) $CD4^+$
936 effector/memory (Teff) cells (sorted as in Extended Data Fig. 9a) from spleens of transferred B6.*Rag1*$^{-}$
937 $^{/-}$ mice over time.
938
939 **Extended Data Figure 9. CAR is required for anti-CD3-induced IL-10 expression in mucosal**
940 **effector and regulatory T cell subsets and suppresses Th17 cell accumulation in the *Rag*$^{-/-}$ transfer**
941 **model. (a)** *Top row*, expression of Foxp3 and RORγt, determined by intracellular staining after *ex vivo*
942 (PMA+ionomycin) stimulation, in $CD4^+CD44^{hi}$ cells from spleen (*left*) or small intestine lamina propria
943 (siLP, *right*) of wild type (B6, blue) or CAR-deficient (B6.*Nr1i3*$^{-/-}$, red) mice injected with or without
944 isotype control (IgG) or anti-CD3 antibody. *Bottom 4 rows*, expression of IL-10 and IL-17A in wild type
945 or CAR-deficient spleen or siLP T cell subsets from mice treated +/- isotype control (IgG) or anti-CD3
946 antibodies. Cells were gated and analyzed by flow cytometry as above. Numbers indicate percentages;
947 representative of 3 mice per group and genotype analyzed over 2-independent experiments. **(b-c)** Mean
948 percentages of IL-10-expressing T cell subsets (± SEM; n = 3), gated and analyzed by *ex vivo* flow
949 cytometry as in (a), in spleen **(b)** or siLP **(c)** T_H cell subsets from wild type (B6, blue) or CAR-deficient
950 (B6.*Nr1i3*$^{-/-}$, red) mice injected with or without isotype control (IgG) or anti-CD3 antibody. * $P < .05$,
951 one-unpaired student's t test; some P values are listed directly. **(d)** Expression of RORγt and IL-17A,
952 determined by intracellular FACS analysis as in Extended Data Figure 8a, in wild type (B6) or CAR-
953 deficient (B6.*Nr1i3*$^{-/-}$) $CD4^+$ effector/memory (Teff) cells from tissues of reconstituted *Rag1*$^{-/-}$ mice 2-
954 weeks post-mixed T cell transfer. Numbers indicate percentages; representative of 5 mice per tissue and
955 time point. **(e)** Mean percentages of (± SEM; n = 5) of wild type (B6; blue) or CAR-deficient (B6.*Nr1i3*$^{-}$
956 $^{/-}$; red) $ROR\gamma t^+IL\text{-}17A^-$ Teff cells, determined by intracellular flow cytometry as in (a). * $P < .05$, paired
957 two-tailed student's t test. **(f)** Expression of RORγt and IL-17A, determined by intracellular FACS
958 analysis, in wild type (B6) or *Il10* $^{-/-}$ Teff cells from tissues of reconstituted *Rag1*$^{-/-}$ mice 2-weeks post-
959 mixed T cell transfer. Numbers indicate percentages; representative of 5 mice per tissue and time point.
960 **(g)** Mean percentages of (± SEM; n = 7) of wild type (B6; blue) or *Il10* $^{-/-}$ (red) $ROR\gamma t^+IL\text{-}17A^-$ Teff
961 cells, determined by intracellular flow cytometry as in (c). * $P < .05$, ** $P < .01$, paired two-tailed
962 student's t test. MLN, mesenteric lymph nodes; siLP, small intestine lamina propria; cLP, colon lamina
963 propria.
964

965 **Extended Data Figure 10. TCPOBOP protection against bile acid-induced ileitis requires CAR**
966 **expression in T cells. (a)** Mean weight loss (± SEM; n = 5/group) of co-housed B6.*Rag2*$^{-/-}$ mice
967 transplanted with CAR-deficient (B6.*Nr1i3*$^{-/-}$) CD4^{+} naïve T cells and maintained on a CA-supplemented
968 diet with or without TC treatment. Weights are shown relative to 3-weeks post-transfer when TC
969 treatments were initiated. NS, not significant; two-way ANOVA. **(b)** H&E-stained sections of terminal
970 ilea or colons from B6.*Rag2*$^{-/-}$ mice reconstituted with CAR-deficient T cells and treated as above and
971 as indicated. Representative of 5 mice/group. **(c)** Mean histology scores (± SEM) for colons or terminal
972 ilea as in (b). NS, not significant; paired student's t test.
973

974 **References**

975

976 1 Hofmann, A. F. & Hagey, L. R. Key discoveries in bile acid chemistry and biology and their
977 clinical applications: history of the last eight decades. *Journal of lipid research* **55**, 1553-1595,
978 doi:10.1194/jlr.R049437 (2014).

979 2 Poupon, R., Chazouilleres, O. & Poupon, R. E. Chronic cholestatic diseases. *J Hepatol* **32**, 129-
980 140 (2000).

981 3 Arab, J. P., Karpen, S. J., Dawson, P. A., Arrese, M. & Trauner, M. Bile acids and nonalcoholic
982 fatty liver disease: Molecular insights and therapeutic perspectives. *Hepatology* **65**, 350-362,
983 doi:10.1002/hep.28709 (2017).

984 4 Cao, W. *et al.* The Xenobiotic Transporter Mdr1 Enforces T Cell Homeostasis in the Presence of
985 Intestinal Bile Acids. *Immunity* **47**, 1182-1196 e1110, doi:10.1016/j.immuni.2017.11.012
986 (2017).

987 5 Lazar, M. A. Maturing of the nuclear receptor family. *J Clin Invest* **127**, 1123-1125,
988 doi:10.1172/JCI92949 (2017).

989 6 Ludescher, C. *et al.* Detection of activity of P-glycoprotein in human tumour samples using
990 rhodamine 123. *British journal of haematology* **82**, 161-168 (1992).

991 7 Pols, T. W., Noriega, L. G., Nomura, M., Auwerx, J. & Schoonjans, K. The bile acid membrane
992 receptor TGR5 as an emerging target in metabolism and inflammation. *J Hepatol* **54**, 1263-1272,
993 doi:10.1016/j.jhep.2010.12.004 (2011).

994 8 Zhang, J., Huang, W., Qatanani, M., Evans, R. M. & Moore, D. D. The constitutive androstane
995 receptor and pregnane X receptor function coordinately to prevent bile acid-induced
996 hepatotoxicity. *J Biol Chem* **279**, 49517-49522, doi:10.1074/jbc.M409041200 (2004).

997 9 Cerveny, L. *et al.* Valproic acid induces CYP3A4 and MDR1 gene expression by activation of
998 constitutive androstane receptor and pregnane X receptor pathways. *Drug Metab Dispos* **35**,
999 1032-1041, doi:10.1124/dmd.106.014456 (2007).

1000 10 Wei, P., Zhang, J., Egan-Hafley, M., Liang, S. & Moore, D. D. The nuclear receptor CAR
1001 mediates specific xenobiotic induction of drug metabolism. *Nature* **407**, 920-923,
1002 doi:10.1038/35038112 (2000).

1003 11 Evans, R. M. & Mangelsdorf, D. J. Nuclear Receptors, RXR, and the Big Bang. *Cell* **157**, 255-
1004 266, doi:10.1016/j.cell.2014.03.012 (2014).

1005 12 Staudinger, J. L. *et al.* The nuclear receptor PXR is a lithocholic acid sensor that protects against
1006 liver toxicity. *Proc Natl Acad Sci U S A* **98**, 3369-3374, doi:10.1073/pnas.051551698 (2001).

1007 13 Ostanin, D. V. *et al.* T cell transfer model of chronic colitis: concepts, considerations, and tricks
1008 of the trade. *American journal of physiology. Gastrointestinal and liver physiology* **296**, G135-
1009 146, doi:10.1152/ajpgi.90462.2008 (2009).
1010 14 Arnold, M. A. *et al.* Colesevelam and Colestipol: Novel Medication Resins in the Gastrointestinal
1011 Tract. *The American journal of surgical pathology*, doi:10.1097/PAS.0000000000000260
1012 (2014).
1013 15 Dawson, P. A., Lan, T. & Rao, A. Bile acid transporters. *Journal of lipid research* **50**, 2340-
1014 2357, doi:10.1194/jlr.R900012-JLR200 (2009).
1015 16 Cui, J. Y. & Klaassen, C. D. RNA-Seq reveals common and unique PXR- and CAR-target gene
1016 signatures in the mouse liver transcriptome. *Biochim Biophys Acta* **1859**, 1198-1217,
1017 doi:10.1016/j.bbagrm.2016.04.010 (2016).
1018 17 Niu, B. *et al.* In vivo genome-wide binding interactions of mouse and human constitutive
1019 androstane receptors reveal novel gene targets. *Nucleic Acids Res* **46**, 8385-8403,
1020 doi:10.1093/nar/gky692 (2018).
1021 18 De Calisto, J. *et al.* T-cell homing to the gut mucosa: general concepts and methodological
1022 considerations. *Methods Mol Biol* **757**, 411-434, doi:10.1007/978-1-61779-166-6_24 (2012).
1023 19 Maglich, J. M. *et al.* Identification of a novel human constitutive androstane receptor (CAR)
1024 agonist and its use in the identification of CAR target genes. *J Biol Chem* **278**, 17277-17283,
1025 doi:10.1074/jbc.M300138200 (2003).
1026 20 Ramesh, R. *et al.* Pro-inflammatory human Th17 cells selectively express P-glycoprotein and are
1027 refractory to glucocorticoids. *J Exp Med* **211**, 89-104, doi:10.1084/jem.20130301 (2014).
1028 21 Moore, L. B. *et al.* Pregnane X receptor (PXR), constitutive androstane receptor (CAR), and
1029 benzoate X receptor (BXR) define three pharmacologically distinct classes of nuclear receptors.
1030 *Mol Endocrinol* **16**, 977-986, doi:10.1210/mend.16.5.0828 (2002).
1031 22 Karwacz, K. *et al.* Critical role of IRF1 and BATF in forming chromatin landscape during type
1032 1 regulatory cell differentiation. *Nat Immunol* **18**, 412-421, doi:10.1038/ni.3683 (2017).
1033 23 Gagliani, N. *et al.* Coexpression of CD49b and LAG-3 identifies human and mouse T regulatory
1034 type 1 cells. *Nat Med* **19**, 739-746, doi:10.1038/nm.3179 (2013).
1035 24 Maynard, C. L. *et al.* Regulatory T cells expressing interleukin 10 develop from Foxp3+ and
1036 Foxp3- precursor cells in the absence of interleukin 10. *Nat Immunol* **8**, 931-941,
1037 doi:10.1038/ni1504 (2007).

1038 25 Barrat, F. J. *et al.* In vitro generation of interleukin 10-producing regulatory CD4(+) T cells is
1039 induced by immunosuppressive drugs and inhibited by T helper type 1 (Th1)- and Th2-inducing
1040 cytokines. *J Exp Med* **195**, 603-616, doi:10.1084/jem.20011629 (2002).
1041 26 Korn, T., Bettelli, E., Oukka, M. & Kuchroo, V. K. IL-17 and Th17 Cells. *Annu Rev Immunol*
1042 **27**, 485-517, doi:10.1146/annurev.immunol.021908.132710 (2009).
1043 27 Sano, T. *et al.* An IL-23R/IL-22 Circuit Regulates Epithelial Serum Amyloid A to Promote Local
1044 Effector Th17 Responses. *Cell* **163**, 381-393, doi:10.1016/j.cell.2015.08.061 (2015).
1045 28 Wan, Q. *et al.* Cytokine signals through PI-3 kinase pathway modulate Th17 cytokine production
1046 by CCR6+ human memory T cells. *J Exp Med* **208**, 1875-1887, doi:10.1084/jem.20102516
1047 (2011).
1048 29 Campbell, C. *et al.* Bacterial metabolism of bile acids promotes generation of peripheral
1049 regulatory T cells. *Nature* **581**, 475-479, doi:10.1038/s41586-020-2193-0 (2020).
1050 30 Song, X. *et al.* Microbial bile acid metabolites modulate gut RORgamma(+) regulatory T cell
1051 homeostasis. *Nature* **577**, 410-415, doi:10.1038/s41586-019-1865-0 (2020).
1052 31 Kim, J. J., Shajib, M. S., Manocha, M. M. & Khan, W. I. Investigating intestinal inflammation
1053 in DSS-induced model of IBD. *J Vis Exp*, doi:10.3791/3678 (2012).
1054 32 Berg, D. J. *et al.* Enterocolitis and colon cancer in interleukin-10-deficient mice are associated
1055 with aberrant cytokine production and CD4(+) TH1-like responses. *J Clin Invest* **98**, 1010-1020,
1056 doi:10.1172/JCI118861 (1996).
1057 33 Langmead, B. & Salzberg, S. L. Fast gapped-read alignment with Bowtie 2. *Nature methods* **9**,
1058 357-359, doi:10.1038/nmeth.1923 (2012).
1059 34 Zhang, Y. *et al.* Model-based analysis of ChIP-Seq (MACS). *Genome Biol* **9**, R137,
1060 doi:10.1186/gb-2008-9-9-r137 (2008).
1061 35 Robinson, J. T. *et al.* Integrative genomics viewer. *Nat Biotechnol* **29**, 24-26,
1062 doi:10.1038/nbt.1754 (2011).
1063 36 Durant, L. *et al.* Diverse targets of the transcription factor STAT3 contribute to T cell
1064 pathogenicity and homeostasis. *Immunity* **32**, 605-615, doi:10.1016/j.immuni.2010.05.003
1065 (2010).
1066 37 Ritchie, M. E. *et al.* limma powers differential expression analyses for RNA-sequencing and
1067 microarray studies. *Nucleic Acids Res* **43**, e47, doi:10.1093/nar/gkv007 (2015).
1068 38 Wei, G. *et al.* Global mapping of H3K4me3 and H3K27me3 reveals specificity and plasticity in
1069 lineage fate determination of differentiating CD4+ T cells. *Immunity* **30**, 155-167,
1070 doi:10.1016/j.immuni.2008.12.009 (2009).

1071 39 Yusuf, I. *et al.* Germinal center T follicular helper cell IL-4 production is dependent on signaling
1072 lymphocytic activation molecule receptor (CD150). *Journal of immunology* **185**, 190-202,
1073 doi:10.4049/jimmunol.0903505 (2010).
1074 40 Suino, K. *et al.* The nuclear xenobiotic receptor CAR: structural determinants of constitutive
1075 activation and heterodimerization. *Mol Cell* **16**, 893-905, doi:10.1016/j.molcel.2004.11.036
1076 (2004).

Figure 1

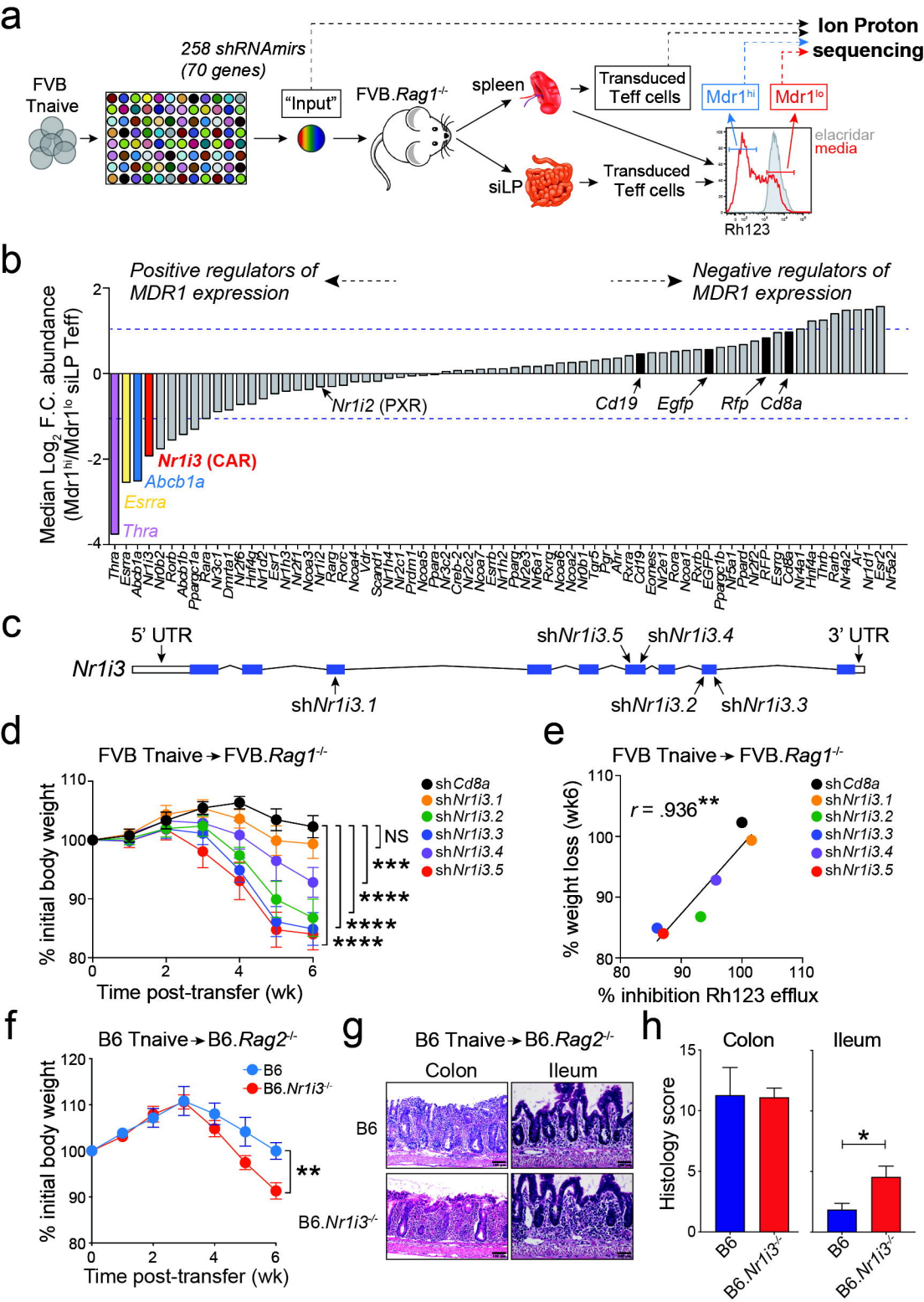
a
Ion Proton sequencing
258 shRNAmirs (70 genes)
FVB Tnaive
"Input"
FVB.Rag1-/-
spleen
siLP
Transduced Teff cells
Transduced Teff cells
Mdr1hi
Mdr1lo
elacridar
media
Rh123
b
Positive regulators of MDR1 expression
Negative regulators of MDR1 expression
Median Log2 F.C. abundance (Mdr1hi/Mdr1lo siLP Teff)
Nr1i2 (PXR)
Cd19
Egfp
Rfp
Cd8a
Nr1i3 (CAR)
Abcb1a
Esrra
Thra
c
5' UTR
3' UTR
Nr1i3
shNr1i3.1
shNr1i3.2
shNr1i3.3
shNr1i3.4
shNr1i3.5
d
FVB Tnaive → FVB.Rag1-/-
% initial body weight
Time post-transfer (wk)
shCd8a
shNr1i3.1
shNr1i3.2
shNr1i3.3
shNr1i3.4
shNr1i3.5
NS
***
****
****
****
e
FVB Tnaive → FVB.Rag1-/-
r = .936**
% weight loss (wk6)
% inhibition Rh123 efflux
f
B6 Tnaive → B6.Rag2-/-
B6
B6.Nr1i3-/-
**
% initial body weight
Time post-transfer (wk)
g
B6 Tnaive → B6.Rag2-/-
Colon
Ileum
B6
B6.Nr1i3-/-
h
Colon
Ileum
Histology score
*
B6
B6.Nr1i3-/-

Figure 2

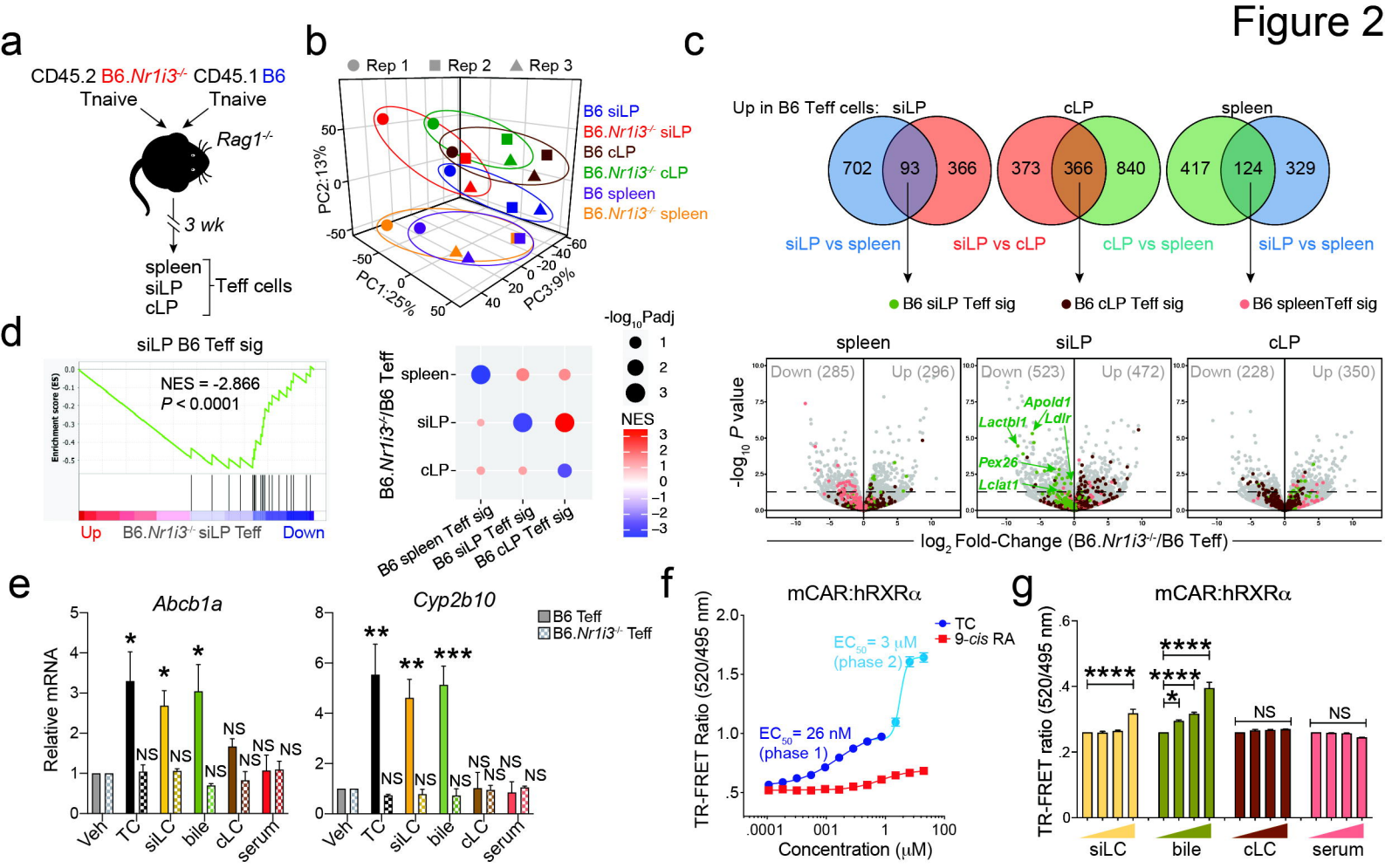
a
CD45.2 B6.Nr1i3-/- CD45.1 B6
Tnaive
Tnaive
Rag1-/-
3 wk
spleen
siLP
cLP
Teff cells
b
Rep 1
Rep 2
Rep 3
B6 siLP
B6.Nr1i3-/- siLP
B6 cLP
B6.Nr1i3-/- cLP
B6 spleen
B6.Nr1i3-/- spleen
PC2:13%
PC1:25%
PC3:9%
c
Up in B6 Teff cells:
siLP
cLP
spleen
702
93
366
373
366
840
417
124
329
siLP vs spleen
siLP vs cLP
cLP vs spleen
siLP vs spleen
B6 siLP Teff sig
B6 cLP Teff sig
B6 spleenTeff sig
spleen
siLP
cLP
Down (285)
Up (296)
Down (523)
Up (472)
Down (228)
Up (350)
Apold1
Lactbl1
Ldlr
Pex26
Lclat1
-log10 P value
log2 Fold-Change (B6.Nr1i3-/-/B6 Teff)
d
siLP B6 Teff sig
NES = -2.866
P < 0.0001
Enrichment score (ES)
Up
B6.Nr1i3-/- siLP Teff
Down
B6.Nr1i3-/-/B6 Teff
spleen
siLP
cLP
B6 spleen Teff sig
B6 siLP Teff sig
B6 cLP Teff sig
-log10Padj
NES
e
Abcb1a
Cyp2b10
Relative mRNA
B6 Teff
B6.Nr1i3-/- Teff
Veh
TC
siLC
bile
cLC
serum
NS
f
mCAR:hRXRα
TC
9-cis RA
EC50= 3 μM
(phase 2)
EC50= 26 nM
(phase 1)
TR-FRET Ratio (520/495 nm)
Concentration (μM)
g
mCAR:hRXRα
TR-FRET ratio (520/495 nm)
siLC
bile
cLC
serum

Figure 3

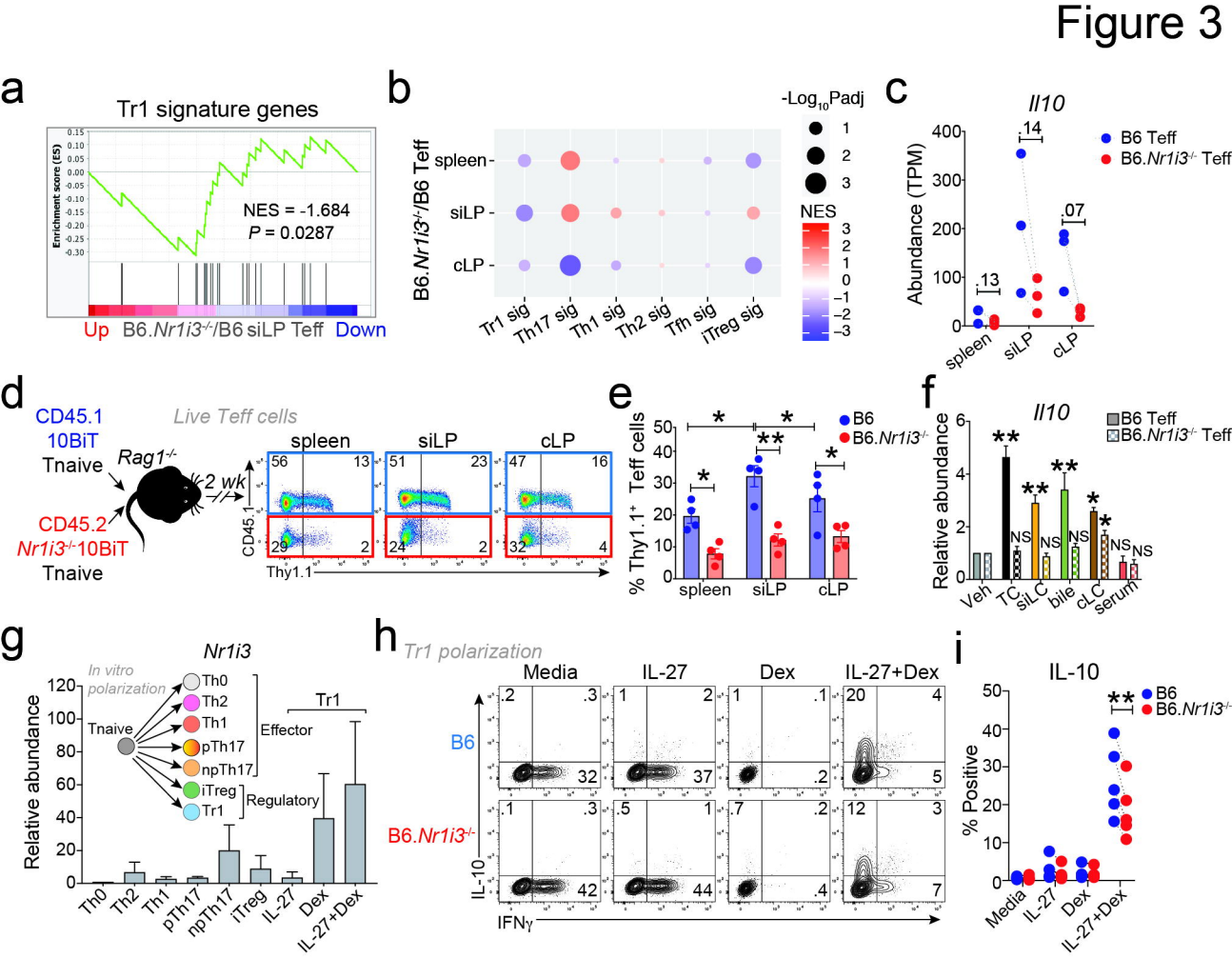
a
Tr1 signature genes
Enrichment score (ES)
NES = -1.684
P = 0.0287
Up
B6.Nr1i3-/-/B6 siLP Teff
Down
b
-Log10Padj
1
2
3
NES
B6.Nr1i3-/-/B6 Teff
spleen
siLP
cLP
Tr1 sig
Th17 sig
Th1 sig
Th2 sig
Tfh sig
iTreg sig
c
Il10
Abundance (TPM)
B6 Teff
B6.Nr1i3-/- Teff
.14
.07
.13
spleen
siLP
cLP
d
CD45.1
10BiT
Tnaive
Rag1-/-
2 wk
CD45.2
Nr1i3-/-10BiT
Tnaive
Live Teff cells
spleen
siLP
cLP
CD45.1
Thy1.1
56
13
29
2
51
23
24
2
47
16
32
4
e
% Thy1.1+ Teff cells
B6
B6.Nr1i3-/-
spleen
siLP
cLP
f
Il10
Relative abundance
B6 Teff
B6.Nr1i3-/- Teff
Veh
TC
siLC
bile
cLC
serum
NS
g
Nr1i3
In vitro polarization
Tnaive
Th0
Th2
Th1
pTh17
npTh17
iTreg
Tr1
Effector
Regulatory
Relative abundance
Th0
Th2
Th1
pTh17
npTh17
iTreg
IL-27
Dex
IL-27+Dex
h
Tr1 polarization
Media
IL-27
Dex
IL-27+Dex
B6
B6.Nr1i3-/-
IL-10
IFNγ
i
IL-10
% Positive
B6
B6.Nr1i3-/-
Media
IL-27
Dex
IL-27+Dex

Figure 4

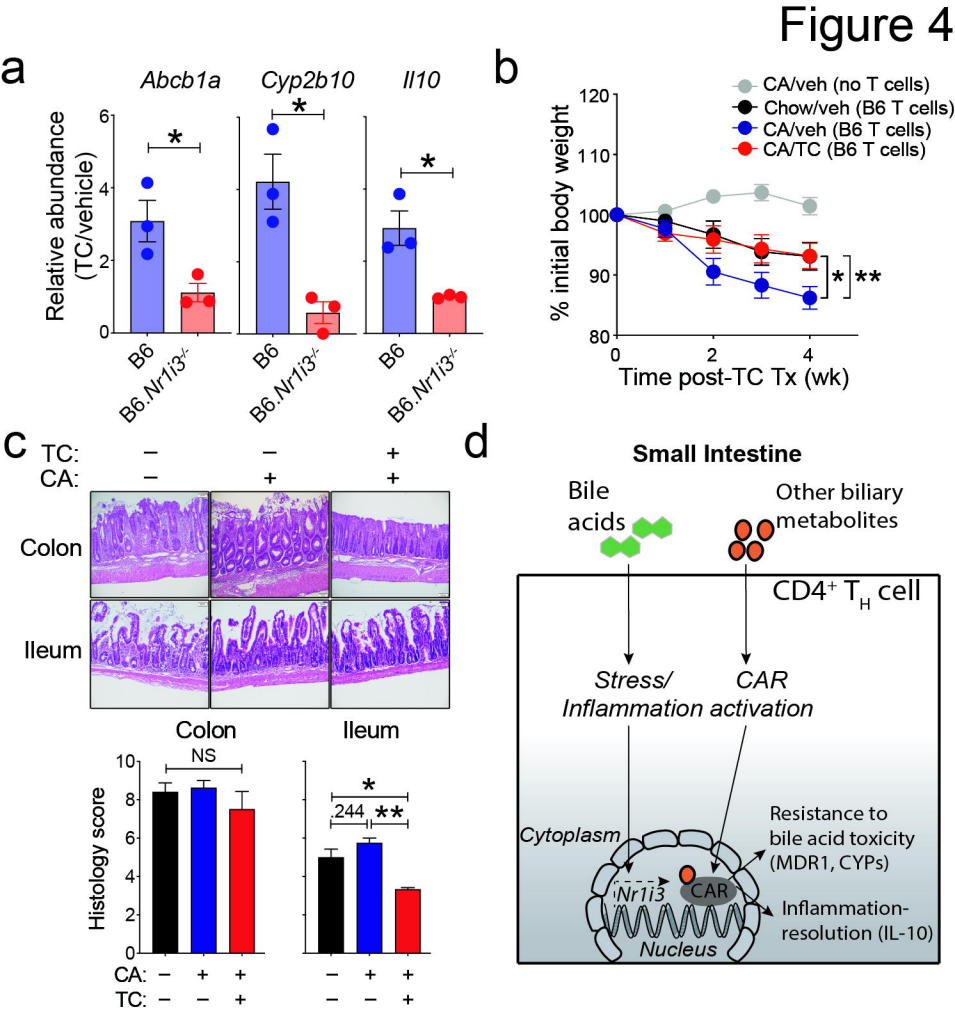
a
Abcb1a
Cyp2b10
Il10
Relative abundance (TC/vehicle)
B6
B6.Nr1i3-/-
b
CA/veh (no T cells)
Chow/veh (B6 T cells)
CA/veh (B6 T cells)
CA/TC (B6 T cells)
% initial body weight
Time post-TC Tx (wk)
c
TC:
CA:
Colon
Ileum
Histology score
NS
244
d
Small Intestine
Bile acids
Other biliary metabolites
CD4+ TH cell
Stress/ Inflammation
CAR activation
Cytoplasm
Nr1i3
CAR
Nucleus
Resistance to bile acid toxicity (MDR1, CYPs)
Inflammation-resolution (IL-10)